



HAL
open science

Uncertainty analysis in model parameters regionalization: a case study involving the SWAT model in Mediterranean catchments (Southern France)

H. Sellami, I. La Jeunesse, S. Benabdallah, N. Baghdadi, M. Vanclooster

► To cite this version:

H. Sellami, I. La Jeunesse, S. Benabdallah, N. Baghdadi, M. Vanclooster. Uncertainty analysis in model parameters regionalization: a case study involving the SWAT model in Mediterranean catchments (Southern France). *Hydrology and Earth System Sciences*, 2014, 18, p. 2393 - p. 2413. 10.5194/hess-18-2393-2014 . hal-01058919

HAL Id: hal-01058919

<https://hal.science/hal-01058919>

Submitted on 28 Aug 2014

HAL is a multi-disciplinary open access archive for the deposit and dissemination of scientific research documents, whether they are published or not. The documents may come from teaching and research institutions in France or abroad, or from public or private research centers.

L'archive ouverte pluridisciplinaire **HAL**, est destinée au dépôt et à la diffusion de documents scientifiques de niveau recherche, publiés ou non, émanant des établissements d'enseignement et de recherche français ou étrangers, des laboratoires publics ou privés.

1 **Uncertainty analysis in model parameters regionalization:** 2 **A case study involving the SWAT model in Mediterranean** 3 **catchments (Southern France)**

4
5 **H. Sellami¹, I. La Jeunesse^{2,3}, S. Benabdallah⁴, N. Baghdadi⁵ and M.**
6 **Vanclooster¹**

7 ¹Earth and Life Institute, Université catholique de Louvain, Croix du Sud 2, Box 2, B-1348
8 Louvain-la-Neuve, Belgium.

9 ²UMR 6173 CITERES, Université de Tours, 33 allée Ferdinand de Lesseps BP 60449 - 37204
10 Tours cedex 3, France.

11 ³LETG-Angers LEESA, UMR 6554 CNRS, University of Angers, Faculty of Sciences 2 Bd
12 Lavoisier, F-49045 Angers Cedex1. France.

13 ⁴Centre de Recherches et des Technologies des Eaux, Technopole Borj Cedria, BP 273,
14 Soliman 8020, Tunisia.

15 ⁵IRSTEA, UMR TETIS, 500 rue François Breton, 34093 Montpellier cedex 5, France

16 Correspondence to: H. Sellami (haysellami@yahoo.fr)

17

18 **Abstract**

19 In this study a method for propagating the hydrological model uncertainty in discharge
20 predictions of ungauged Mediterranean catchments using a model parameter regionalization
21 approach is presented. The method is developed and tested for the Thau catchment located in
22 southern France using the SWAT hydrological model. Regionalization of model parameters
23 based on physical similarity measured between gauged and ungauged catchments attributes is
24 a popular methodology for discharge prediction in ungauged basins, but it is often confronted
25 with an arbitrary criterion for selecting the “behavioral” model parameters sets (Mps) at the
26 gauged catchment. A more objective method is provided in this paper where the transferrable
27 Mps are selected based on the similarity between the donor and the receptor catchments. In
28 addition, the method allows propagating the modeling uncertainty while transferring the Mps

1 to the ungauged catchments. Results indicate that physically similar catchments located
2 within the same geographic and climatic region may exhibit similar hydrological behavior and
3 can also be affected by similar model prediction uncertainty. Furthermore, the results suggest
4 that model prediction uncertainty at the ungauged catchment increases as the dissimilarity
5 between the donor and the receptor catchments increases. The methodology presented in this
6 paper can be replicated and used in regionalization of any hydrological model parameters for
7 estimating streamflow at ungauged catchment.

8 **1 Introduction**

9 Hydrological models are generally calibrated against observation variable(s), typically
10 streamflow, to estimate some parameters that cannot be measured directly and to achieve a
11 reliable prediction of the watershed response. However, in many cases, observed streamflow
12 data are not available or are insufficient. Therefore, the catchment is considered as ungauged
13 (Sivapalan et al., 2003) which may undermine the planning and the management of the water
14 resources in the ungauged catchment. To overcome this problem, various regionalization
15 techniques have been developed to estimate streamflow in ungauged catchments including
16 methods based on similarity approach (Vandewiele and Elias, 1995; Idrissi et al., 1999; Merz
17 and Blöschl, 2004; McIntyre et al., 2005; Oudin et al., 2008) and/or statistical approach
18 (Sivapalan et al., 2003; Yadav et al., 2007). The latter approach consists of deriving statistical
19 relationships between catchment attributes (CAs), such as topography, soil, drainage area,
20 etc., and the optimized model parameters (Mps). Once these relationships have been
21 established, one can determine the parameters of an ungauged basin using its CAs. Although
22 it can be considered as the most common regionalization approach for ungauged catchment
23 (Wagener and Wheater, 2006), statistical approaches were deeply criticized due to the
24 assumption that most statistical models consider linearity between CAs and optimized Mps
25 (Merz and Blöschl, 2004 ; Parajka et al., 2005; McIntyre et al., 2005). On the other hand,
26 regionalization based on similarity approach consists of transferring the information from
27 donor catchment(s) to receptor catchment(s). It starts by identifying one or more donor
28 catchments which are usually gauged catchments and that are most likely to be hydrologically
29 similar to one or more receptor catchments. Then, transfer the relevant information (Mps or
30 streamflow records) from donor to receptor catchments. Typically, Mps transfer from donor
31 to receptor catchment(s) rely on physical similarity measures. In this case, the same CAs as
32 used in the statistical technique can be adopted to identify similar catchments. Alternatively,

1 use can be made of spatial proximity measures (e.g. the distance between the centroids of the
2 catchments). The similarity regionalization approach is lying on the assumption that similar
3 catchments behave hydrologically similarly. So, the definition of the similarity measure,
4 certainly subjective, will condition the success of the selected regionalization approach
5 (Heuvelmans et al., 2006).

6 Several studies have focused on the transfer of Mps based on similarity approach for
7 predicting streamflow records at ungauged catchments (Merz and Blöschl, 2004; McIntyre et
8 al., 2005; Parajka et al., 2005; Bårdossy, 2007; Oudin, et al., 2008). For instance, McIntyre et
9 al., (2005) found that Mps transfer outperformed as compared to the statistical regression
10 approach using a five parameters version of the Probability Distribution Model (Moore, 1985)
11 applied on 127 UK catchments. Similar conclusions were drawn by Oudin et al., (2008) using
12 two conceptual rainfall-runoff models on 913 French catchments; the GR4J (modèle du Génie
13 Rural à 4 paramètres Journalier) developed by Perrin et al. (2003) and the TOPMO model
14 which is a six parameters version of the TOPMODEL (Beven, 1997). Parajka et al. (2005)
15 have used 4 groups of regionalization approaches. The first group is based on spatial
16 averaging of calibrated model parameters, the second is based on spatial proximity (spatial
17 distance) between the catchments, the third uses multiple regression between catchments
18 attributes and model parameters and the last group is based on similarity between catchment
19 attributes. They have found that regionalization methods based on spatial proximity and
20 catchment attributes similarity performed better than multiple regression and spatial averaging
21 methods. However, other studies have reported that even nearby catchments can be
22 hydrologically different (Ouarda et al., 2001; Shu and Burn (2003); McIntyre et al., 2005;
23 Beven, 2000).

24 The similarity approach for regionalization of Mps in ungauged catchments implies the
25 “good” performance of the calibrated hydrological model at the donor catchment. Then, Mps
26 that lead to “good” or “behavioral” model simulations are selected and transferred to the
27 ungauged catchment. However, it is argued that hydrological model predictions, even in well
28 gauged catchments are subject to inherent uncertainty that stems from different uncertainty
29 sources (e.g. inputs, parameter uncertainty, model structure, and observed data). Because of
30 all these uncertainty sources, it is expected and argued that model calibration will lead to non-
31 unique sets of parameters (Beven and Binley, 1992). Therefore, it becomes difficult to
32 associate the calibrated parameters with the physical characteristics of the catchment.

1 While model parameters uncertainty at well gauged catchment has received considerable
2 attention during the past two decades (Beven and Binley 1992, Duan et al., 1992; Abbaspour
3 et al., 1997; Muleta and Nicklow, 2005; Vrugt et al., 2008; Yang et al., 2008; Zhang et al.,
4 2009, Shen et al., 2012), a little attention has been given to the uncertainty resulting from Mps
5 regionalization at the ungauged sites (Wagener and Wheater, 2006). Furthermore, additional
6 uncertainty related to the regionalization procedure that stems from the arbitrary choices of
7 the CAs, the similarity measure, the selection of the candidate parameter sets to be transferred
8 can have a significant effect on the model prediction uncertainty in the ungauged catchments.
9 Addressing all these sources of uncertainty and understanding the way they can affect the
10 model prediction in the ungauged catchment is a challenging task (Sivapalan et al., 2003 and
11 Wagener et al., 2004).

12 This paper aims to contribute to this challenge by addressing the following question: how can
13 Mps uncertainty of donor catchments be propagated through regionalization schemes based
14 on the similarity approach, and how does it affect the prediction uncertainty in ungauged
15 catchment? Specific questions are: (1) Is the selected hydrological model suitable for
16 reproducing the hydrology in the ungauged catchment? (2) How does parameter uncertainty
17 affect model prediction uncertainty in the ungauged catchment through the regionalization
18 scheme?

19 In an attempt to answer to these research questions, the paper is organized in 3 main sections.
20 In the first section the study site, the data available, the modeling approach and the
21 regionalization procedure are described. The second section describes and discusses the
22 results of the modeling and the regionalization approach. The final section reports the main
23 outcomes of the paper as a summary and conclusions.

24 **2 Study site description and available data**

25 **2.1 Study site description**

26 The Thau catchment is located on the French Mediterranean coast (Languedoc-Rousillon
27 region) and drains an area of approximately 280 Km². The catchment is drained by ten
28 streams that flow directly into the lagoon (Fig.1). The basins size varies from 3.42 Km² to 67
29 Km² with the biggest one corresponding to the Vène catchment. Other geomorphologic and
30 topographic characteristics of these catchments are given in Table 2. Dominant land use types

1 are vineyards and non-agriculture vegetation (trees, Mediterranean sclerophyllous vegetation).
2 The distribution of the main land use within each sub-catchment is given in Table 2. The
3 eastern part of the Thau catchment area is composed of Jurassic limestone overlaid by
4 Miocene marls in its central part, corresponding to 60% of the Vène watershed surface. These
5 Jurassic limestone are characterized by the presence of a large karstic aquifer whose limits
6 extend the topographic limit of the catchment and strongly influences the hydrological regime
7 of the Vène catchment (Plus et al., 2006; Gallart et al., 2008; Perrin and Tournoud, 2009;
8 Sellami et al., 2013). Soils in this part of the Thau catchment are mainly sandy-loam and silty-
9 loam soils with porosity ranging from 35 to 50 % at 1 m depth of the soil profile. The western
10 part of the Thau catchment is composed of the Eocene marls overlaid mainly by the Miocene
11 marls. This region covers the central part of the Pallas, Aygues_Vacques, Nègues_Vacques,
12 Mayroual, Soupié and Fontanilles catchments with silty-clayey-loam and loam textured soils
13 so that runoff generation process are expected to be different from the eastern part.

14 **2.2 Available data**

15 The climate is a typical Mediterranean regime characterized by a large seasonal variability of
16 rainfall in time and space with an annual average value of 600 mm. Precipitation occurs as
17 short intense storms mainly during autumn and spring (from September to January) and
18 separated by a long dry period (from February to August). The hottest months are July and
19 August where the maximum temperature can exceed 35°C and the coldest months are
20 December and January where daily minimum temperature can reach -5°C.

21 Data such as a Digital Elevation Model (50 m grid, provided by the French National
22 Geographic Institute), a soil map (50 m resolution, provided by the INRA Montpellier) and
23 land use maps (50 m resolution) for 1996 (La Jeunesse et al., 2002) and 2010 are available for
24 each catchment. Daily precipitation data (from 1990 to 1999) are provided by five rain gauge
25 stations located within the study area (Fig.1) but only the Sète rain gauge (French national
26 meteorological station of Météo France) has daily precipitation data from 1990 to 2009. Daily
27 temperatures are provided from the meteorological station of Sète. Wind speed, air relative
28 humidity and solar radiation daily data are provided from the meteorological station of
29 Fréjorgues airport located 20 km in the northeastern of the Thau catchment.

30 In the Thau basin about two years (1994-1996) streamflow records are available for the Vène
31 and the Pallas catchments, while for the other rivers, streamflow records are either missing or

1 either have missing values and are not long enough to allow direct model calibration. The
2 lengths of the available streamflow records, as well as their corresponding time periods, for
3 each catchment are summarized in Table 1. Such a case of poorly gauged catchments is very
4 common in semi-arid and Mediterranean area and, when coupled with discontinuities in flow
5 regime of ephemeral rivers, makes the modeling of the discharge challenging.

6 Although observed streamflow time series are available for some catchments but are at
7 different time periods (1994-1996 and 2007-2009), climate characteristics (mean daily/annual
8 precipitation, mean, maximum and minimum daily temperature, etc.) between these two time
9 periods are relatively similar. However, land use and land cover (LULC) types between the
10 time periods have undergone a slight change according to the LULC map of 1996 and 2010.
11 Figure 2 shows the change of LULC occurred in the Pallas and in the Vène catchments
12 between 1996 and 2010. It shows that vineyards surface have decreased by an average of 13%
13 whereas non-agriculture vegetation has increased by an average of 7%. Despite that, it is well
14 argued that LULC is one of the major drivers of the hydrological processes and catchment
15 runoff response (Nathan and McMahon, 1990; Wagener et al., 2007). The study of the effect
16 of land use change on model parameters regionalization approach results is, however, not
17 within the objectives of this paper.

18 As the Pallas and the Vène catchments have been subject to many previous studies (Aquilina
19 et al., 2002; La Jeunesse et al., 2002; Plus et al., 2006; Chahinian et al., 2011, Sellami et al.,
20 2013) more detailed data are available for these subcatchments. Therefore, the Vène and the
21 Pallas catchments are considered as gauged catchments, while all the other small catchments
22 are considered ungauged.

23 **3 Description of the hydrological model**

24 The Soil and Water Assessment Tool (SWAT) (Arnold et al., 1998) is a continuous-time and
25 physically based hydrological model. SWAT is developed to predict the impact of land
26 management practices on water, sediment and agricultural chemical yields in large complex
27 catchments with different soil, land use and management conditions over long periods of time
28 (Eckhardt et al., 2005). The hydrological model operates by dividing the watershed into
29 subbasins. Each subbasin is further discretized into a series of hydrologic response units
30 (HRUs), which are unique soil-land use combinations. Soil water content, surface runoff,
31 nutrient cycles, sediment yield, crop growth and management practices are simulated for each

1 HRU and then aggregated for the subbasin by a weighted average. The hydrological balance
2 is calculated based on the following equation:

$$3 \quad \frac{\partial SW}{\partial t} = P_{day} - Q_{surf} - E_a - W_{seep} - Q_{gw} \quad (1)$$

4 where SW is the soil water content (mm), P_{day} is precipitation rate (mm/day), Q_{surf} is the
5 surface runoff rate (mm/day), E_a is evapotranspiration rate (mm/day), W_{seep} is the water
6 percolation rate from the soil profile (mm/day), and Q_{gw} is the groundwater flow rate
7 (mm/day).

8 The water in each HRU in SWAT is stored in four storage volumes: snow, soil profile,
9 shallow aquifer, and deep aquifer. Surface runoff from daily rainfall is estimated using a
10 modified SCS curve number method, which estimates the amount of runoff based on local
11 land use, soil type, and antecedent moisture condition. Calculated flow, sediment yield, and
12 nutrient loading obtained for each subbasin are then routed through the river channel using the
13 variable storage or Muskingum method. The watershed concentration time is estimated using
14 Manning's Kinematic Equation, considering both overland and channel flow.

15 The soil profile is subdivided into multiple layers that support soil water processes including
16 infiltration, evaporation, plant uptake, lateral flow, and percolation to lower layers. The soil
17 percolation component of SWAT uses a water storage capacity technique to predict flow
18 through each soil layer in the root zone. Downward flow occurs when field capacity of a soil
19 layer is exceeded and the layer below is not saturated. Percolation from the bottom of the soil
20 profile recharges the shallow aquifer. The amount of water entering the shallow aquifer is a
21 function of the total water volume exiting the soil profile and an exponential decay function to
22 account for the recharge time delay. The latter is depending on the overlying geologic
23 formations. If the depth of the shallow aquifer increases above the user defined threshold
24 value, it is assumed that groundwater discharge is occurring and contributing to the reach.
25 Upward flow movement to the overlaying unsaturated soil layers is simulated by routing
26 water in the shallow aquifer storage component to the soil by capillary pressure or by direct
27 absorption by the plant roots. This remove water process is termed "revap".

28 The model computes evaporation from soils and plants separately. Potential
29 evapotranspiration can be modelled with three options available in SWAT, that is, Penman-
30 Monteith, Priestley-Taylor and Hargreaves methods (Neitsch et al., 2005), depending on data

1 availability. Potential soil water evaporation is estimated as a function of potential ET and
2 leaf area index. Actual soil evaporation is estimated by using exponential functions of soil
3 depth and water content. Plant water evaporation is simulated as a linear function of potential
4 ET, leaf area index, and root depth, and can be limited by soil water content. More detailed
5 descriptions of the SWAT model can be found in Neitsch et al., (2005).

6 The SWAT simulations are conducted on the gauged catchments from 1990 to 1996 on a
7 daily time step. However, due to the complex nature of the flow processes and the presence of
8 the karstic system in the catchment, a model warm-up period of 4 years (1990-1993) is
9 considered to be sufficient to minimize the effects of the initial state of the SWAT variables
10 on the river flow prediction (Sellami et al., 2013). The modified SCS curve number method is
11 chosen for surface runoff volume computing. The variable storage coefficient method is
12 selected for the flow routing through the channel and potential evapotranspiration is estimated
13 by the Penman-Monteith method. The daily stream flow data from 02/08/1994 to 01/07/1996
14 and from 25/11/1995 to 14/06/1996 for the Vène and the Pallas catchments, respectively, are
15 used to assess the model prediction performances.

16 **4 Modeling approach**

17 **4.1 Sensitivity analysis (SA)**

18 A way to deal with high-dimensional hydrological models, such as SWAT, is to conduct SA
19 to select only the sensitive model parameters that are assumed to represent the real system
20 behavior. In the current study case, a SA is conducted using the built-in SWAT SA tool that
21 uses the Latin Hypercube One-factor-AT-a Time (LH-OAT) (van Griensven et al., 2006)
22 method. In the LH-OAT technique only one input parameter is modified between two
23 successive model runs. Therefore, the change in model output can then be attributed to such
24 parameter modification. In this study, parameter that induces the highest model output change
25 is ranked first and the less sensitive parameter is given a rank equals to zero. A complete
26 detailed explanation of this SA technique can be found in van Griensven et al., (2006).

27 SA is performed on 17 SWAT model parameters that may have a potential to influence the
28 flow river (Table 3). Snow parameters are not included in the SA since the study site belongs
29 to a semi-arid climate and the flow is not affected by the snow melt process. The ranges of
30 parameters variation are based on the SWAT manual (Neitsch et al., 2005) and are sampled

1 by considering a uniform distribution (Yang et al., 2008; Chahinian et al., 2011) in their
2 physical range. Ten sensitive SWAT parameters are identified for each of the Pallas and the
3 Vène catchment (Table 3). The identified sensitive parameters are the same for both cases but
4 they differ in their ranking. The first two ranked parameters are groundwater related
5 parameters: ALPHA_BF (a parameter that expresses the recession or the rate at which the
6 groundwater is returned to the flow) and GWQMN (a threshold depth of water in the shallow
7 aquifer required to return flow). The third ranked parameter for the Vène river is
8 GW_DELAY, which is defined as the required time for water leaving the bottom of the root
9 zone to reach the shallow aquifer where it can contribute to lateral groundwater flow. This
10 groundwater parameter is ranked 7th for the Pallas river. The third ranked parameter for the
11 Pallas river is CN2, which is the initial SCS runoff curve number for moisture condition and
12 that determines the volume of surface runoff contributing to the total stream flow. This latter
13 parameter is a surface runoff parameter that depends on several factors including soil types,
14 soil textures, soil permeability, land use properties, etc. The remaining sensitive parameters
15 for the Vène and the Pallas catchments are direct or indirect surface runoff related parameters:
16 CH_K, which is the hydraulic conductivity of the channel; CH_N, which is the manning's
17 value of the tributary channel; ESCO, which is the soil evaporation compensation factor
18 which directly influences the evapotranspiration losses from the watershed; EPCO, which is
19 the plant uptake compensation factor and expresses the amount of water needed to meet the
20 plant uptake demand; GW_REVAP, which is dimensionless coefficient controlling the rate of
21 water movement between the root zone and the shallow aquifer; and SURLAG, which
22 controls the fraction of the total water that is allowed to enter the stream on any specific day.

23 It is argued that in order to provide better identified models and to ensure high regionalization
24 potential, the structure of the selected hydrological model should be reduced to only
25 components that describe the key process of the system. Therefore, it is suggested that the
26 number of required model parameter should not be more than half a dozen (Wagener et al.,
27 2001). However, the approach to retain only the necessary model structure components
28 (parsimonious model) do not necessary guarantees that all the hydrological processes of the
29 watershed are identified and represented, especially in complex hydrological systems.
30 However, from the results of the SA and the physical meaning of the selected sensitive
31 parameters it is obviously difficult to select less than 10 parameters in the current study. In
32 addition, it is well known that the hydrological processes are complex in the study area due to
33 the presence of the karstic aquifer in the Vène watershed (Plus et al. 2006, Gallart et al. 2008,

1 Perrin and Tournoud 2009, Chahinian et al. 2011). Hence, selecting the 10 sensitive
2 parameters described above ensures that the model does not omit one or more hydrological
3 processes important for this particular case study. Furthermore, other studies dealing with the
4 SWAT model have identified more or less 10 sensitive parameters that are assumed to
5 describe appropriately the hydrological process of the real system. For example, Heuvelmans
6 et al., (2004) have identified 7 sensitive SWAT model parameters related to flow generation
7 to be regionalized in Northern Belgium. Gitau and Chaubey (2010) have selected 16 SWAT
8 parameters for flow prediction in ungauged catchments. Chahinian et al., (2011) have
9 calibrated 14 SWAT model parameters for modeling flow and nutrient emission processes.
10 They found that 12 sensitive parameters are directly and indirectly related to flow simulation.

11 **4.2 Uncertainty analysis (UA)**

12 The Generalized Likelihood Uncertainty Estimation, GLUE, (Beven and Binley 1992) is
13 selected for assessing the model parameter uncertainty. The reasons behind selecting this
14 technique are its simple concept, its relative ease of implementation and use without major
15 modifications to the method itself. GLUE is a Monte Carlo based method for modelling
16 uncertainty analysis (Beven and Binley, 1992; Freer et al., 1996 for details). The approach is
17 based on a large number of model runs with different combinations of the parameter values
18 chosen randomly and independently from the prior distribution of the parameter space. By
19 comparing predicted and observed responses, each set of parameter values is assigned a
20 likelihood value which is a function that quantifies how well that particular parameter
21 combination simulates the observed system. Based on a cutoff threshold, the total sample of
22 simulations is then split into “behavioral” and “non-behavioral” parameter combinations.
23 Then, from the cumulative distribution of the model predictions the desired quantiles are
24 computed to represent the uncertainty bands. Therefore, the selection of these quantiles has an
25 impact on the parameter uncertainty analysis (Blasone et al., 2008; Xiong and O’Connor,
26 2008; Jin et al., 2010; Gong et al., 2011). However, it is very common that the 95%
27 confidence interval is used to represent the prediction uncertainty interval which is also used
28 in this study. Others subjective choices are considered within the implementation of the
29 GLUE framework in this study. The prior distributions of the selected parameters are assumed
30 to follow a uniform distribution over their respective range (Table 3). This initial distribution
31 is chosen since the real distribution of the parameter is unknown. The ranges of the
32 parameters are chosen based on the SWAT manual (Neitsch et al., 2005) and previous

1 applications of the technique with the SWAT model (Yang et al., 2008; Shen et al., 2012). To
 2 sample the prior parameter distribution, a simple random sampling is implemented. The
 3 number of sampling sets is set to 10,000. Such number of simulations was identified as
 4 sufficient for assessing uncertainty of about 10 sensitive SWAT model parameters (Yang et
 5 al., 2008, Gong et al., 2011). Moreover, it was mentioned by Yang et al. (2008) that no
 6 significant change was observed in the GLUE results between 10,000 and 20,000 model runs.
 7 So, the selected number of 10,000 simulations is considered reasonably sufficient for this
 8 study. The likelihood function selected is the Nash and Sutcliffe (1970) efficiency coefficient
 9 (NS) since it is widely used as a likelihood measure within GLUE in the literature (Beven and
 10 Freer, 2001; Arabi et al., 2007; Shen et al., 2012).

$$11 \quad NS = 1 - \frac{\sum_{i=1}^n (P_i - O_i)^2}{\sum_{i=1}^n (O_i - \bar{O})^2} \quad (2)$$

12 with O_i is the observed value, \bar{O} mean observed values and P_i is the predicted value. The
 13 range of NS lies between 1 (perfect fit) and $-\infty$.

14 The cutoff threshold selected to separate “behavioral” from “non-behavioral” parameter sets
 15 is another subjective choice within the GLUE method. Frequently, when the likelihood value
 16 is greater than zero the corresponding simulations are considered “behavioral” (Freni et al.,
 17 2010; Gong et al., 2011). In this study, model simulations with negative NS values are
 18 considered unacceptable and, therefore, the corresponding parameter sets are discarded from
 19 further analysis. The selection of the threshold value is an entirely arbitrary choice that affects
 20 the prediction uncertainty (Montanari, 2005; Mantovan and Todini, 2006) and probably is the
 21 most important concern for the GLUE method. A small cutoff threshold will lead to larger
 22 “behavioral” simulations and larger uncertainty bands, while larger threshold value will
 23 decrease the numbers of “behavioral” models and will reduce the uncertainty interval width
 24 (Xiong and O’Connor, 2008; Blasone et al., 2008; Viola et al., 2009). As the GLUE method is
 25 dependent on all these subjective decisions that influence the final uncertainty prediction, it
 26 has been deeply criticized and its several drawbacks have been well pointed out and discussed
 27 in the literature (Montanari, 2005; Mantovan and Todini, 2006).

1 **4.3 The regionalization schemes**

2 The adopted regionalization method for this study is the transfer of Mps from donor to
3 receptor catchment based on the similarity between their physical attributes (topography,
4 geology, soils, drainage area, etc.). The physical similarity approach is based on the
5 assumption that catchment physiographic characteristics predetermine the hydrological
6 behavior. Therefore, the selection of relevant CAs is crucial for the success of the
7 regionalization procedure. The catchments attributes (CAs) selected and used to define
8 similarity are related to topography, land cover, drainage area, soil and geology features
9 (Table 2). They are derived from the available data such as land use maps, soil maps, digital
10 elevation model and geology maps. These CAs are generally considered as the main drivers
11 of the hydrological process in the literature (Merz and Blöschl, 2004; Heuvelmans et al.,
12 2006; Wagener et al., 2007; Bastola et al., 2008) and are the most common ones used to
13 define similarity between catchments in model parameter regionalization schemes. For
14 instance, Heuvelmans et al. (2006) have considered catchment area, average slope, dominant
15 land use and soil texture classes as the most appropriate catchment descriptors in model
16 parameters regionalization in Flemish part of the Scheldt river basin (Belgium). Besides these
17 CAs, others authors have used flow indices or characteristics using flow duration curve (FDC)
18 such as (Masih et al., 2010), indices of hydrological responses (Yadav et al., 2007) or hydro-
19 meteorological long term data (Bastola et al., 2008) as relevant catchment descriptors.
20 However, the selection of the appropriate CAs depends also on the physical meaning of the
21 selected model parameters, on the objective of the regionalization procedure and on the
22 knowledge about the key hydrological processes occurring within the catchment. For
23 example, when the objective of the regionalization procedure is to estimate the flow in
24 ungauged catchments, as in our case, the use of flow characteristics or indices as input is
25 useless. Model parameters, especially those of physically based model such as SWAT, are
26 assumed to be closely related to CAs and, thus, representing the functional behavior of the
27 catchment response. For instance, in the SWAT model the curve number parameter (CN2)
28 depends on the soil and land use characteristics of the catchment which are considered among
29 the relevant catchment descriptors. Knowledge about the key processes in the system can also
30 assist the selection of the relevant CAs. As an example, the geology is considered as relevant
31 catchment descriptor in our study case since it is known that the Jurassic limestone aquifer in
32 the eastern part of the Thau catchment strongly influences the hydrological regime of the
33 Vène catchment (Sellami et al., 2013).

1 Within each catchment, the dominant soil physical texture based on the relative proportion of
2 sand, silt and clay is considered to identify the CAs related to soil type. The main geological
3 features considered is the surface catchment percentage covered by the Jurassic limestone
4 estimated using the GIS tools based on a simplified geological map of the Thau catchment.
5 Other geomorphologic and topographic descriptors (mean elevation, mean slope, drainage
6 area) are also calculated using GIS tools and are reported in Table 2. Besides the CAs, it is
7 very common that climatic characteristics such as long-term precipitation characteristics, the
8 annual precipitation, annual potential evapotranspiration index, solar radiation, etc. (see,
9 Wagener et al., 2007), are used for the similarity measure between the catchments. However,
10 in our case study such climatic descriptors are omitted since we are dealing with small and
11 geographically close catchments located within a relatively small area under the same climate
12 regime.

13 Unfortunately, there does not exist a universally accepted metric or combination of metrics to
14 quantify catchments similarity in the catchment attributes dimension. Some authors have used
15 the inverse of the Euclidean distance (Heuvelmans et al., 2004) or the normalized sum of the
16 absolute difference (Parajka et al., 2005). Others authors (Masih et al., 2010) have used the
17 weighted normalized sum of the absolute difference where equal or more weights are assigned
18 to individual catchment attributes in order to consider their varying assumed importance. To
19 identify similar catchments groups, each catchment is assigned to its own cluster and the
20 similarity matrix between clusters, in the catchment attributes dimension, is calculated. Then,
21 clusters with the largest similarity measure are linked together into binary clusters based on
22 the average linkage method where the distance between two clusters is defined as the average
23 distance between all objects belonging to these clusters. These steps are repeated and the
24 similarity matrix between clusters is updated until all clusters are linked together in a
25 hierarchical tree. The Pearson's correlation coefficient, denoted hereafter as R^2 , is used as a
26 similarity metric between catchments attributes; the higher the R^2 between the target and the
27 donor catchments, the more similar they are. Once the clusters are established, information
28 can be transposed from donor(s) to receptor(s) catchment(s). In complex hydrological models
29 this transfer of information is a difficult task due to the parameter uncertainty, to their
30 interdependency, to the non-unique solution and to other various sources of uncertainty
31 (Bárdossy, 2007). Some authors (Heuvelmans et al., 2004; McIntyre et al., 2005; Bárdossy
32 2007; Oudin et al., 2008; He et al., 2011) suggest to transfer the entire parameter sets to the
33 ungauged catchment(s) justifying that transferring the entire parameter sets does not interfere

1 with the integrity of the model parameters as a set and that the entire hydrological processes
2 are considered at once.

3 The traditional way of transferring the Mps from donor(s) to receptor(s) catchment(s) can also
4 be based on the selection of the “behavioral” Mps obtained from simulations with likelihood
5 values (e.g. NS index) above certain user defined threshold value at the donor(s)
6 catchment(s). However, doing this way all the receptor(s) catchment(s) will receive equal
7 number of Mps despite that they are not equally similar to the donor(s) catchment(s). This
8 may overestimate the prediction uncertainty at the closest receptor(s) catchment(s) and may
9 underestimate it at catchments that are further from the donor(s) catchment(s). Furthermore,
10 the selection of the “behavioral” Mps is often based on an arbitrary and entirely subjective
11 choice of a threshold value which may add to the uncertainty of the final regionalization
12 results.

13 In this section we propose a more objective method for selecting the appropriate Mps to be
14 transferred from the gauged to the ungauged catchment. First, the similarity measure ($R^2_{(d,r)}$)
15 between gauged and ungauged catchment in their CAs dimension is calculated (data not
16 shown) and clusters with similar catchments are constructed. The SWAT model is
17 implemented and parameterized at each catchment based on the SWAT pre-processing
18 procedure with the available data while model parameter calibration and uncertainty analysis
19 are conducted only at the gauged catchments (donor catchments) using the GLUE approach.
20 At this stage, only Mps sets that lead to positive NS values between observation and model
21 simulation at the gauged catchment are retained. Based on the similarity measure and the
22 maximum NS value, a new threshold value, denoted hereafter *Thresh*, is calculated and
23 updated using Eq.(3) that serves as a cutoff value to identify the candidates Mps to be
24 transferred from the donor to the receptor catchment.

$$25 \quad Thresh_{(d,r)} = R^2_{(d,r)} \times \max NS_d \quad (3)$$

26 where $R^2_{(d,r)}$ is the similarity measure between the donor catchment (d) and the receptor
27 catchment (r) and scaled between 0 and 1, and NS_d is the highest likelihood value reached in
28 the model simulations at the donor catchment (d). To compute the threshold value
29 ($Thresh_{(d,r)}$), the similarity matrix between all catchments attributes is calculated (data not
30 shown). By applying Eq. (3) the number of the candidate Mps will increase linearly as the
31 dissimilarity between the donor(s) and the receptor(s) catchment(s) increases. Furthermore,
32 besides parameter uncertainty, additional uncertainty related to the regionalization schemes is

1 explicitly accounted in the final model prediction at the ungauged catchment(s) by
 2 introducing the similarity measure in Eq.(3). As the dissimilarity between the donor(s) and the
 3 target catchment(s) increases, model prediction uncertainty in the target catchment(s)
 4 intuitively increases and vice versa. Another advantage of using Eq.(3) is that the selection of
 5 the threshold value to define the number of the candidate Mps is based on the similarity
 6 metric rather than on a subjective choice of the modeler which may reduce this additional
 7 uncertainty component in the final regionalization procedure. Once the threshold value
 8 (*Thresh*) is calculated the entire selected Mps are transferred from the donor catchment(s) to
 9 the receptor(s) catchment(s).

10 Because updating manually the parameter values in the text SWAT file is a time consuming
 11 and tedious task, a sampling and rewriting program in the MATLAB® computing language
 12 was developed that provides the Mps from the donor catchment to the receptor catchment in
 13 the SWAT model format.

14 **4.4 Modeling evaluation criteria**

15 Besides the NS statistical criteria the correlation coefficient R^2 is used to assess the goodness
 16 of fit between observation and the SWAT model simulations. The Model prediction
 17 uncertainty is quantified by the *p-factor* which is the percentage of measured data bracketed
 18 by the 95% prediction uncertainty (95PPU) and by a measure of the Average Relative Interval
 19 Length *ARIL* proposed by Jin et al., (2010). However, for more efficient comparison between
 20 the ungauged catchments without observations data, the *ARIL* was modified by standardizing
 21 the upper and lower boundary values of the simulated point by its mean value. The modified
 22 *ARIL* is called, hereafter, the Average Standardized Relative Interval Length (*ASRIL*).

$$23 \quad p_factor = \frac{NQ_{in}}{n} \times 100 \quad (4)$$

$$24 \quad ASRIL = \frac{1}{m} \sum_{t=1}^m \frac{Q_{t,97.5\%}^M - Q_{t,2.5\%}^M}{Mean(Q_t^M)} \quad (5)$$

25 where NQ_{in} is the number of observed discharge falling in the 95PPU , $Q_{t,97.5\%}^M$ and $Q_{t,2.5\%}^M$
 26 represent the upper and lower simulated boundary, respectively, at time t of the 95PPU, n is
 27 the number of observation data points, m is the length of simulation , the subscript M refers to
 28 simulated, t refers to the simulation time step. The goodness of calibration and prediction

1 uncertainty is judged on the basis of the closeness of the *p-factor* to 100% (i.e., all
2 observations are bracketed by the 95PPU) and the *ASRIL* to 0 (if there is no uncertainty, the
3 value of *ASRIL* is zero). A smaller value of *ASRIL* and higher value of *p-factor* represent
4 better performance.

5 To assess the relative performances of the regionalization procedure for flow estimation in
6 ungauged catchments, usually the simulated flow is compared to the observed one and/or
7 sometimes gauged catchments are considered in turn as if they are ungauged (Oudin et al.,
8 2008). In the current work, catchments have very scarce streamflow records. Therefore any
9 available observation data, field knowledge and/or previous work conducted in the area of
10 interest can be precious and helpful to check the performance of the adopted regionalization
11 method. Performance assessment of the regionalization procedure is based on three evaluation
12 criteria. The first one namely fit to observation (van Griensven et al., 2012) and consists of
13 the quantitative assessment of model accuracy simulations compared to measurements using
14 some statistical criteria. In this regard, the simulated FDCs flow percentiles are compared to
15 the observed ones by using the NS coefficient and the model prediction uncertainty is
16 assessed through the *p-factor* (percentage of observed data bracketed in the 95% uncertainty
17 interval) wherever observation data are available. The second one is called fit to reality (van
18 Griensven et al., 2012) and consists of the evaluation of the model capability in reproducing
19 the real hydrological process and in reflecting the reality of the field. For instance, the
20 predicted mass balance can be calculated and used to assess the performance of the
21 regionalization procedure in representing the main hydrological processes that govern the
22 hydrology of the study system. The third evaluation criterion is called fit to geography and it
23 consists of mapping the predicted variable in order to check the soundness of its spatial
24 distribution with some observed data (e.g. soil moisture maps) or with some field knowledge
25 (e.g. geology, karstic system, etc.).

26 **5 Results and discussions**

27 **5.1 Model performances and prediction uncertainty at the gauged catchments**

28 The NS values range from 0 to 0.71 with an average value of 0.47 for the Vène catchment
29 while they range from 0 to 0.76 with an average value of 0.60 for the Pallas catchment. The
30 correlation coefficient (R^2) is higher than 0.80 in both catchments indicating that SWAT is
31 able to satisfactorily reproduce the general behavior of the observed hydrograph of both

1 watersheds. The GLUE parameter sets are more robust and consistent in providing
2 simulations that match better the observations of the Pallas catchment than these of the Vène
3 catchment.

4 The 95% GLUE prediction interval (95PPU) is considered for uncertainty analysis. The
5 average width of the 95PPU is evaluated using the *ASRIL* and the percentage of data
6 bracketed by this interval is estimated using the *p-factor*. The 95% GLUE uncertainty interval
7 for the Vène and the Pallas catchments is plotted in Fig. 3. The *ASRIL* and the *p-factor* are
8 2.48 and 70% for the Pallas catchment, while the same statistics are 2.75 and 63% for the
9 Vène catchment, respectively. The statistics are far from their suggested values (*ASRIL* ≈ 0
10 and *p-factor* $\approx 100\%$) indicating wide prediction uncertainty for both catchments. The reasons
11 can be attributed to the several uncertainty sources (e.g. input data, parameter uncertainty,
12 model structure uncertainty, error in the measured data, etc.) and to the subjectivity in the
13 GLUE method (e.g. threshold value, the likelihood function, the initial parameter distribution)
14 involved at each modelling step (Xiong and O'Connor, 2008; Shrestha et al., 2009).
15 Furthermore, the karstic nature of the study site (especially the Vène catchment) makes the
16 discharge modelling using the SWAT model more challenging and more uncertain (Sellami et
17 al., 2013).

18 Besides the model prediction uncertainty, the parameters correlation and posterior distribution
19 are investigated (results not shown). It is noted that different GLUE parameter combinations
20 lead to similar model results in both case study. This is known as the equifinality concept
21 (Beven and Binley, 1992) which is behind the GLUE method philosophy. Equifinality
22 originates from the imperfect knowledge of the system under consideration and from different
23 error sources (errors in input and boundaries conditions, errors in using an approximate model
24 structure of the real system and error in the observation variable being modelled) that can
25 interact in a non-linear way (Beven, 2006). In addition, some parameters depicted as very
26 sensitive by the SA method turned out to be less sensitive or less important by the GLUE
27 method, such as ALPHA_BF and GWQMN. In fact, given the equifinality behind the GLUE
28 concept and the possible correlations and interactions between parameters, a single parameter
29 may lose in importance in the context of a combination of parameters values. As a corollary,
30 GLUE cannot reveal the sensitivity of a single parameter.

31 The posterior parameters distribution (PDs) derived from the Monte Carlo runs are large and
32 rather uniformly distributed over their range. This is because GLUE tends to flatten the

1 response surface of the parameter by given equally weight to “behavioral” model runs. These
2 results are consistent with previous studies (e.g. Yang et al., 2008 and Dotto et al., 2012).
3 However, the PDs shape and the uncertainty range of the parameters are dependent on the
4 selected threshold value (Fig.4). By selecting a threshold $NS \geq 0$, all parameters are rather
5 uniformly distributed which lead to non-identifiable parameters indicating wide parameter
6 uncertainty. While increasing the threshold value to $NS = 0.60$, some parameter PDs become
7 narrower and peakier and well identified. This is illustrated in Fig.4 for the example of the
8 CN2 and GW_DELAY for the Vène catchment, and CN2 and SURLAG parameters for the
9 Pallas catchment. In addition to the shape of the parameter PDs, increasing the threshold
10 value results in a decline of the numbers of “behavioral” Mps retained and causes the
11 depletion of the coverage of the observation by the uncertainty interval. For instance, by
12 selecting a threshold value $NS \geq 0.60$, the *p-factor* decreased from 70% to 46% and from 63%
13 to 53% for the Pallas and the Vène catchments, respectively. The *ASRIL* also decreased to
14 2.23 and to 1.92 in the Vène and in the Pallas catchments, respectively, following the increase
15 of the threshold value. These results are in accordance with the findings of Blasone et al.,
16 (2008) and Gong et al., (2011) and suggest that interpretation of parameter uncertainty
17 derived by GLUE is always conditioned to the choices of threshold value and the prediction
18 uncertainty level.

19 Investigations of the parameters correlation matrices (data not shown) show very low
20 correlation between the parameters. It seems that GLUE does not explicitly account for
21 parameters interaction. Many authors (Blasone et al., 2008; Yang et al., 2008; Jin et al., 2010)
22 have reported the weak correlation between parameters within the GLUE method. One
23 explanation can be that the selected sampling strategy cannot account for parameters
24 interaction since each parameter is individually randomly sampled from its distribution.

25 **5.2 Results of the regionalization approach**

26 **5.2.1 Catchments clustering**

27 The similarity metric based on the multidimensional space of CAs resulted into 4 ungauged
28 catchments similar to the Vène catchment (Lauze, Aiguilles, Joncas and Mayroual) and 4
29 ungauged catchments similar to the Pallas catchment (Fontanilles, Aiguilles,
30 Nègues_Vacques and Soupié). Catchments within the same group are assumed to have similar
31 hydrological behavior. The catchments clusters and the numbers of the candidate Mps

1 transferred from the donor to the receptor catchments, calculated using the similarity measure,
2 are given in Table 4. The Vène and the Pallas catchment are identified as the donor
3 catchments while all the others ungauged watersheds are considered as receptor catchments.
4 The highest threshold value (*Thresh*) calculated using Eq. (3) is $Thresh = 0.50$ and 0.66 for
5 the Vène and the Pallas catchment, respectively. These *Thresh* values are frequently used in
6 literature to identify “behavioral” Mps (Gassman et al., 2007, Shen et al., 2012). The lowest
7 *Thresh* values range between 0.25 and 0.38 corresponding to a transfer of 89.18% and of
8 96.52% of the total Mps sets of the Vène and the Pallas catchments, respectively (Table 4).
9 These *Thresh* values correspond to poor model performances at the gauged catchments and
10 can be seen as low compared to what has been usually used in literature. However, as it was
11 reported by Oudin et al., (2008), it is not straightforward to state whether or not poorly
12 modeled gauged catchment(s) parameters should be transferred to ungauged catchment(s).
13 From one side, it is expected that Mps associated with poorly modeled hydrographs in gauged
14 catchment(s) will yield poor model performances at the ungauged catchment(s). On the other
15 side, transfer of Mps of poorly modeled gauged catchment(s) may add a diversity which can
16 be beneficial for modeling the ungauged catchment (Oudin et al., 2008).

17 **5.2.2 Predicted Flow Duration Curves (FDCs) at the ungauged catchments**

18 The FDC provides the percentage of time (duration) a daily or monthly (or some other time
19 interval) streamflow is exceeded over a period for a particular river basin (Castellarin et al.,
20 2004). FDC may also be viewed as the complement of the cumulative distribution function of
21 the considered streamflow and is probably one of the most informative methods of displaying
22 the complete range of river discharges, from low flows to flood events. Empirical FDCs can
23 be easily constructed from streamflow observations using standardized non-parametric
24 procedures (see Vogel and Fennessey, 1994, 1995; Smakhtin, 2001; Castellarin et al., 2004).
25 The FDC concerns only the flow magnitude whereas the streamflow time series concerns both
26 magnitude and time sequence. The flow percentiles conceptually represent different segments
27 of the FDC: high flow ($\leq Q_{10}$), median flows (Q_{10} - Q_{50}) and low flows (Q_{50} - Q_{100}). The
28 simulated FDCs resulting from the transfer of the GLUE Mps sets of the Pallas and the Vène
29 catchment to the ungauged catchments, within their corresponding group, are plotted in Fig.5.
30 The slope of the simulated FDCs within the high flow percentiles ($\leq Q_{10}$) is relatively steep
31 for the two catchments groups, indicating that flood discharges are not sustained for a long
32 period of time. The slope of the end tail of the simulated FDCs, corresponding to low flow (\geq

1 Q50), is steeper in the Pallas catchment group, while it is flattened out considerably in the
2 Vène catchments group. This reflects the difference in the low flow regime between the two
3 catchments groups. Catchments of the Pallas group cease flowing at 20% to 40% of the
4 simulation time period, while catchments of the Vène group have more sustained baseflow
5 contribution. Figure 6 shows the coefficient of variation ($CV = \text{Standard deviation}/\text{Mean}$) and
6 the mean magnitude of the simulated FDCs flow percentiles for all the catchments and
7 quantify their inter and intra-catchments groups variability. It is clearly seen from Fig.6 that
8 the CV of the mean for all the FDCs flow percentiles within the Pallas catchments group is
9 higher at low flows than at higher flows while, for the Vène catchments group, the CV is
10 more or less steady across the flow percentiles, except for the Mayroual catchment. The intra-
11 catchments variability of the CV of the flow percentiles within each catchment group shows
12 that catchments within each group converge to a similar low flow CV value, except for the
13 FDCs of the Fontanilles within the Pallas group and the Mayroual within the Vène group. It is
14 worth noting here, that these catchments exhibit the largest dissimilarity in their physical
15 attributes from their corresponding donor catchments. It is also clear in Fig.6 that the
16 simulated mean flow magnitude of the different flow percentiles is very low in both
17 catchments group. The mean values of the high flow percentiles in both catchments group do
18 not exceed $0.015\text{m}^3.\text{s}^{-1}$. However, the variation in the mean values of the simulated FDCs is
19 more important in high flow percentiles than in low flow percentiles in both catchment
20 groups. In the Pallas catchment group, the mean flow magnitude decreases rapidly from Q10
21 to Q20, then progressively from Q20 to Q50 leading to progressive increase in the CV within
22 these flow percentiles and tends to be steady for flow percentile higher than Q50, which
23 results in higher CV values. In addition, at low flow percentiles ($> Q50$), all the simulated
24 FDCs of the Pallas catchment group tend to have similar mean flow values which resulted in
25 less variability of the CV at the low flow percentiles. Also, catchments within the Vène group
26 have much more variability in their simulated flow percentiles mean values than these of the
27 Pallas group. The flow percentiles of the simulated FDCs of the Aiguilles catchment have the
28 highest mean values while the Mayroual and Lauze FDCs flow percentiles are very similar
29 and these of the Joncas catchment are the lowest values. It is worth noting here to add that the
30 CV of low flow percentiles is also compared to the catchments drainage area and to the soil
31 characteristics within each ungauged catchment, but no clear relationships is found.

1 **5.2.3 Uncertainty in the predicted FDCs at the ungauged catchments**

2 The uncertain simulated FDCs are represented in Fig.5 in such a way that dissimilarity
3 between the donor and the receptor catchment, within each catchments group, increases from
4 the left to the right and from top to down. It is clearly seen from Fig.5 that the FDCs
5 uncertainty interval in both catchments groups is wider as the receptor catchment is further
6 from the donor catchment. This is also confirmed by the relationship that exists between the
7 number of Mps transferred from the donor to the receptor catchments and the *ASRIL* factor
8 plotted in Fig.7. The *ASRIL* factor increases as the percentage of the transferred Mps
9 increases. While the average FDCs uncertainty width (*ASRIL*) in both catchments groups
10 tends to increase as the dissimilarity between the donor and the receptor catchments increases,
11 catchments of the Pallas group show wider uncertainty interval than these of the Vène group.
12 Another observation that can be made from Figs. 5 and 7 is that catchments that are very
13 similar to each other have similar uncertain FDCs shape and very close *ASRIL* factor values
14 (see also Table 5). This is the case for the Joncas and Lauze catchments in the Vène group and
15 for the Nègues_Vacques and Aygues_Vacques catchments in the Pallas group. This suggests
16 that high similarity between CAs may lead to similar hydrological responses and model
17 prediction uncertainties of catchments that are under the same climatic and geographic region.
18 However, this assumption is far to be validated in this work and needs to be further
19 investigated and checked in future work with larger number of similar catchments or by
20 simply gauging the catchments.

21 In order to check the consistency of the developed methodology in this work, attempts are
22 conducted to investigate if relationships between parameter uncertainty of the donor
23 catchment and the predicted uncertainty of the FDCs in the receptor catchments exist. This
24 has been done through the calculation of the coefficient of variation (*CV*) of the transferred
25 Mps within each ungauged catchment. The *CV*, as it was described previously, can be used as
26 a dimensionless measure of parameter uncertainty (Bastola et al., 2008). The variability of the
27 *CV* of Mps transferred to the ungauged catchments within each catchment group is given in
28 Fig.8. Results show that the *CV* of Mps varies between the catchments depending on the
29 parameter itself and on the similarity distance between the receptor and the donor catchments.

30 In the Pallas catchment group, the CN2 and the SURLAG parameters show a clear variability
31 in their corresponding *CV* values across the catchments. It is obvious that uncertainty in CN2
32 and SURLAG parameters increases from the closest (Nègues-Vacques) to the furthest

1 ungauged catchment (Fontanilles) from their respective donor catchment (Fig.8a). Moreover,
2 the variability trend of the CV of the CN2 parameter follows closely the trend of the *ASRIL*
3 factor across the catchments, with a correlation coefficient of $R^2= 0.66$ while the CV of the
4 *SURLAG* parameter is less correlated to the *ASRIL* factor ($R^2= 0.40$). In the Vène catchment
5 group, 3 out of 10 transferred parameters show variable CV values across the catchments.
6 These parameters are CN2, GW_DELAY and ALPHA_BF (Fig.8b). While all the other
7 remaining parameters show a constant CV at its maximum value across all the catchments,
8 uncertainty in CN2, GW_DELAY and ALPHA_BF parameters increases progressively from
9 the closest similar ungauged catchment (Joncas) to the furthest one, but in different trends.
10 The variability of the CV of CN2 is well correlated to the *ASRIL* factor ($R^2= 0.83$) while these
11 of the GW_DELAY and ALPHA_BF parameters are less correlated to *ASRIL* ($R^2= 0.545$ and
12 0.540 for GW_DELAY and ALPHA_BF, respectively). These results suggest that
13 relationships exist between the transferred parameter uncertainty and the predicted uncertainty
14 width of the FDCs and between the CAs similarity distance and the predicted uncertainty in
15 the ungauged catchment. The results are consistent with the proposed methodology in this
16 work which is based on the principle that model prediction uncertainty intuitively increases as
17 the dissimilarity in CAs between the donor and the receptor catchments increases. However,
18 these results need to be interpreted with care and precaution. Indeed, the CV is calculated for
19 each model parameter individually without taking simultaneously into account the uncertainty
20 and the interactions between the other parameters while it is the whole parameters set that was
21 transferred in the regionalization schemes. By relating the parameter CV to the model
22 prediction uncertainty in ungauged catchment, it is assumed that linear relationship exists
23 between parameter uncertainty and model prediction uncertainty at the ungauged catchments.
24 However, this linearity is difficult to check and to establish because of the possible
25 interdependency of the parameters, non-linearity and non-monotonicity of the hydrological
26 model and other various sources of uncertainty (uncertainty in input and model structure).
27 Moreover, model parameters that have steady CV across the ungauged catchments may
28 contribute to model prediction uncertainty when they are transferred in a set of parameters.
29 Therefore, the CV of individual parameter may not reflect its real uncertainty. In addition to
30 Mps, input and model structure uncertainty, regionalization procedures are known to have
31 additional uncertainty on model prediction in ungauged catchments (Wagener et al., 2004;
32 Heuvelmans et al., 2006; Bastola et al., 2008). In the proposed methodology it is assumed that
33 uncertainty that stems from the regionalization schemes is propagated to model prediction in

1 the ungauged catchment through the integration of the similarity measure in defining the Mps
2 sets to be transferred from the donor to the receptor catchments. However, partitioning each
3 uncertainty source and telling to which extent it can affect the model prediction is a very
4 difficult task to perform.

5 **5.3 Performances evaluation of the regionalization approach**

6 **5.3.1 Fit to observation**

7 The 95% uncertainty interval and the median of each flow percentiles values of the observed
8 and the simulated FDCs for the ungauged catchments, where observed data are available, are
9 constructed and plotted in Fig.9. Only 4 ungauged catchments have some observed data that
10 can be used to compare the results of the regionalization approach. According to the observed
11 FDCs, ungauged catchments cease flowing at 50 to 60 % of the time while the predicted
12 FDCs indicate that ungauged catchments flow for longer period between 60 and 100% of the
13 simulation time period reflecting the ephemeral hydrological behaviour of the catchments
14 (Fig.9). The calculated NS coefficient between the observed and the simulated median flow
15 percentiles and the average *p-factor* values, corresponding to the average percentage of the
16 observed flow percentile values bracketed in the predicted uncertainty flow percentile
17 interval, are summarized in Table 6. Given the observation data available, the NS coefficient
18 values are negative for the Soupié and Fontanilles catchments (NS = -0.131 and -0.144,
19 respectively), indicating that the observed median values of the different flow percentiles are
20 poorly reproduced by the model in these ungauged catchments. On the other hand, positive
21 NS values of 0.169 and 0.518 are obtained in the Aygues_Vacques and in the Joncas
22 catchments, respectively, showing better model prediction of the flow percentiles median
23 values. While the simulated flow percentiles uncertainty intervals are able to bracket most of
24 the observation data (Fig.9 and Table 6), there is a clear tendency of the *p-factor* increase with
25 the decrease of the distance between the donor and the receptor catchment. As it was
26 demonstrated previously, the average relative width of the uncertainty interval (*ASRIL*)
27 increases as the dissimilarity between the donor and the receptor catchments increases.
28 Therefore, more observation data are bracketed in the flow percentile uncertainty interval of
29 the ungauged catchments that are located far from the donor catchment.

1 **5.3.2 Fit to reality**

2 The annual mass balance is calculated based on the average annual values of the different
3 hydrological components that are computed by the SWAT model according to Eq. (6).

$$4 \text{ WYLD} = \text{Surf_Q} + \text{Lat_Q} + \text{GW_Q} - \text{T Losses} \quad (6)$$

5 Where WYLD is the net water yield to reach (mm), Surf_Q is the surface runoff (mm), Lat_Q
6 is the lateral flow contribution to reach (mm), GW_Q is the groundwater discharge into the
7 reach (mm) and T Losses is the amount of water removed from the tributary channel by
8 transmission (mm). The WYLD decomposes the contribution of the different flow types to the
9 total water budget and is actually equals to precipitation diminished by evapotranspiration.

10 The average annual water budget, its components and their corresponding uncertainty
11 (calculated as the standard deviation) for each ungauged catchment are plotted in Fig.10. The
12 results of the regionalization approach suggest that surface runoff is the major component of
13 the water budget (65% in average) followed by the lateral flow (22.7% in average) and by the
14 groundwater flow (12.3% in average). However, all the hydrological balance components are
15 estimated with large uncertainty. For instance, about 65% of the WYLD uncertainty is
16 attributed to the uncertainty of the estimated surface runoff (Surf_Q). In the SWAT model,
17 Surf_Q is estimated using the modified Soil Conservation Service (SCS) curve number (CN)
18 method which depends on the soil moisture and land use cover. Therefore, any uncertainty in
19 the soil and land use cover is translated to the associated curve number and affects the
20 predicted Surf_Q. Moreover, in SWAT the runoff coefficient is calculated as the ratio of
21 runoff volume to rainfall. Therefore, uncertainty of the latter can affect the predicted peak
22 flow which in turn affects the predicted Surf_Q.

23 The groundwater component (GW_Q) has more important average contribution rate to the
24 total water budget in the Vène catchments group (Joncas, Lauze, Aiguilles and Mayroual)
25 with an average of 11.71%, than in the Pallas catchments group (Nègues_Vacques,
26 Aygues_Vacques, Soupié and Fontanilles), with an average of 6.47%. In addition, GW_Q
27 within the Pallas catchments group occurs intermittently, while it seems more sustained but
28 also more uncertain within the Vène catchments group (Fig.10). Because of the different
29 sources of uncertainty (e.g. precipitation, evapotranspiration, uncertainty in groundwater
30 parameters) and the rainfall seasonal variability, the groundwater volume and its level of
31 fluctuation are estimated with uncertainty that is translated into an uncertain GW_Q. These

1 results suggest that streamflow in the Vène catchments group (corresponding more or less to
2 the eastern part of the Thau catchment, see Fig. 1) is more influenced by the groundwater
3 flow contribution than in the Pallas catchments group (corresponding to the central and
4 western part of the Thau catchment). However, the validation of this result is not
5 straightforward since no information or data on groundwater are available in the study area
6 and more hydrogeological measurements are required to check the results and to reduce the
7 groundwater discharge uncertainty.

8 About 2.5% of the total water budget is lost via leaching through the stream bed (T Losses).
9 This type of losses is more important in the Pallas catchments group (5.3%), than in the Vène
10 catchment group (1.37%) (Fig.10). Transmission losses become more important when GW_Q
11 decreases and vice versa. Because the SWAT model creates more sustained shallow aquifer
12 with larger water storage in the eastern part than in the western part of the Thau catchment,
13 the Vène catchments group are gaining much more water through baseflow (GW_Q + Lat_Q)
14 leading to smaller loss of water through channel transmission. However, besides the depth of
15 water stored in the shallow aquifer, other geomorphologic parameters (e.g. the width and
16 length of the channel bed, etc.) and hydraulic parameters (e.g. effective hydraulic conductivity
17 of the river bed (Ch_K), geologic nature of the channel material) can affect the transmission
18 losses amount. For example, for catchments where the groundwater level is beyond the river
19 bed, the CH_K value should be equal to zero (van Griensven et al., 2012) and should not be
20 too high in humid catchments. Uncertainty in the estimated transmission losses can stem from
21 the uncertainty of the physical features of the catchments introduced through the GIS data and
22 used by SWAT to derive the channel geomorphological characteristics and from the
23 uncertainty of the CH_K parameter.

24 **5.3.3 Fit to geography**

25 This criterion is used here to assess the performances of the regionalization procedure in
26 reproducing the actual spatial distribution of the soil moisture in the Thau catchment.
27 Baghdadi et al. (2012) proposed a method to estimate the volumetric soil moisture from
28 RADARSAT-2 image (space Synthetic Aperture Radar «SAR» sensor) for bare agricultural
29 fields or fields with thin vegetation cover over the Thau basin for ten dates between
30 November 2010 and March 2011. Their estimated soil moisture values showed a good
31 agreement with the measured in situ soil moisture with a RMSE = $0.065 \text{ cm}^3/\text{cm}^3$ (see
32 Baghdadi et al., 2012 for details). These estimated soil moisture maps, referred hereafter as

1 “observed” soil moisture, are compared to the soil moisture derived from the regionalization
2 results which are referred hereafter as predicted soil moisture. Since the “observed” soil
3 moisture maps are available only for three different dates (November 18, December 4 and 12,
4 2010) within the model simulation period, the comparison between the “observed” and the
5 predicted soil moistures is restricted to these 3 dates. Figure 11 shows the spatial distribution
6 of the predicted and the observed soil moisture for three different dates at the Thau catchment.
7 The predicted soil moisture is spatially correlated to the “observed” one but with different
8 degree of satisfaction. The latter can be broadly and arbitrary set to good, satisfactory and
9 poor based on the graphical investigation of Fig.11. Good spatial correlation between the
10 distribution of the predicted and the “observed” soil moisture is obtained at the Vène,
11 Aiguilles and Fontanilles catchments, while it can be considered as satisfactory for the Joncas,
12 Lauze, Pallas and Soupié and poor for the Aygues_Vacques, Mayroual and Nègues_Vacques
13 catchments. Overall, the predicted soil moisture has an acceptable spatial distribution with the
14 “observed” one which is more clear in the eastern part (corresponding to the Vène catchments
15 group) than in the western part (corresponding to the Pallas catchments group) of the Thau
16 catchment.

17 The predicted soil moisture values on the three different dates at the Thau catchment are also
18 compared to the “observed” ones. Table 7 presents some statistical characteristics of the 95%
19 “observed” and predicted soil moisture values on the three selected dates. The predicted soil
20 moisture values ranges are slightly larger than the “observed” ones. The variability of the
21 predicted soil moisture on a given day is larger as this day is preceded by wet days (Table 7).
22 Nevertheless, the median and the mean of the “observed” and predicted soil moisture values
23 are in a good agreement. However, the comparison of the “observed” and predicted soil
24 moisture values is not straightforward since the model is predicting the soil moisture at the
25 HRU scale for soils with different vegetation type cover, while the “observed” soil moisture
26 values are made up for bare soils or soils with thin vegetation cover. In addition, “observed”
27 soil moisture values are made up for the top 5 to 10 cm of the soil profile whereas the
28 predicted ones might be estimating by SWAT for the entire soil layer that can be much more
29 than 10 cm depth.

30 **6 Summary and conclusions**

31 This study examined the possibility of the Soil and Water Assessment Tool (SWAT) model to
32 accurately predict the daily discharge at gauged and ungauged catchments within an

1 uncertainty framework. The model was implemented on a Mediterranean catchment, called
2 the Thau catchment located in southern France. Model calibration and parameters uncertainty
3 were conducted simultaneously using the GLUE method (Beven and Binley, 1992) on two
4 gauged subcatchments of the Thau watershed, referred to as the Vène and the Pallas
5 catchment.

6 We first questioned whether the selected hydrological model is suitable for reproducing the
7 hydrology of the study area. The model showed good performances in reproducing the daily
8 observed discharge of the Vène and the Pallas catchments with NS coefficient higher than
9 0.70. The model was able to cover more than 60% of the observation discharge data of each
10 catchment in its 95% prediction uncertainty interval. However, the model prediction
11 uncertainty was large in both study sites especially in the Vène catchment.

12 We subsequently questioned whether the selected hydrological model is able to predict the
13 discharge at ungauged catchments. We analyzed this question through the transfer of the
14 SWAT model parameter sets from the gauged catchments (Vène and Pallas) to the other
15 ungauged catchments of the Thau watershed. A regionalization approach based on similarity
16 measure between catchments attributes was adopted to identify similar catchments clusters.
17 Within each cluster, the degree of similarity between the donor and the receptor catchment
18 was used as a threshold to select the appropriate transferrable model parameter sets.

19 Results showed that within the same catchments cluster, ungauged catchments can exhibit
20 similar hydrologic behavior if they exhibit high degree of similarity in their physical attributes
21 and have received similar model parameter sets. Similar ungauged catchments showed higher
22 similarity at the predicted FDCs high flow percentiles than at low flow percentiles. The high
23 variability of the predicted low flow values was attributed to the predicted low mean values of
24 the flow percentiles rather than to the geology or to the catchment drainage area.

25 The performance of the regionalization method at the ungauged catchments was assessed
26 through statistical and field reality criteria. The predicted median flow percentiles, given the
27 available observed data, were poorly to acceptable reproduced by the model. The predicted
28 water balance revealed the prevailing of the surface runoff component in the hydrology of the
29 ungauged catchments. The predicted soil moisture was satisfactory spatially correlated to the
30 “observed” one for some given dates. The findings suggest that the SWAT model parameters
31 can be regionalized to predict discharge at ungauged catchments and the results can fit the
32 reality of the study case. However, thorough evaluation and criticism of its performances is

1 constrained by the availability of the observation data at the ungauged catchments. Therefore,
2 other evaluation criteria such as fit to reality and fit to geography can be used to describe the
3 model performances in these ungauged catchments.

4 We also showed in this work how parameter uncertainty can affect model prediction
5 uncertainty at ungauged catchment through the regionalization of the model parameters. The
6 assumptions behind the developed methodology were that physically similar catchments are
7 hydrologically similar and model prediction uncertainty increases as the dissimilarity between
8 the donor and the receptor catchment increases. The developed methodology allows
9 propagating model parameter uncertainty proportionally to the similarity measure.
10 Furthermore, it makes the selection of the donor catchment parameter sets more objective
11 than the traditional approach which is based on modeler subjective choice. It was shown that
12 model prediction uncertainty was influenced by the similarity distance between the donor and
13 the receptor catchment. Wider prediction uncertainty is obtained as the dissimilarity between
14 the donor and the receptor catchment increases. It was also shown that within the same
15 climatic and geographic region, catchments that are very similar to each other and have
16 received similar model parameter sets exhibit similar degree of prediction uncertainty. In
17 addition, the findings showed that the selected threshold values and, hence, the number and
18 the uncertainty of the parameters transferred can affect the prediction uncertainty at the
19 ungauged catchment. If a higher degree of similarity exists between the donor and the
20 receptor catchments then a higher threshold value is selected. Consequently, a lower
21 parameters uncertainty is propagated to the ungauged catchment leading to lower prediction
22 uncertainty in the ungauged catchment. Otherwise, a lower threshold value is selected and a
23 wider uncertain parameter sets are transferred which will yield a larger uncertain model
24 prediction at the target catchment. However, it is not pretended with these results that
25 uncertainty in the transferred parameter sets is the only one source for model prediction
26 uncertainty at the ungauged catchment. As it was demonstrated by the results, although the
27 relationship between uncertainty in the parameters and in the prediction results at the
28 ungauged catchments exists, this relationship is far to be linear. This is due to other sources of
29 uncertainty (e.g. model structure, inputs uncertainty), parameters correlation and equifinality.
30 Therefore, all sources of uncertainty should be considered in an integrated framework for
31 more effective parameter regionalization.

1 To our knowledge, a hydrological study of the entire Thau catchment was never done before.
2 Therefore, building on the regionalization approach, this work can be considered as a starting
3 point for further research study of hydrological issues in this catchment.

4 We think that the developed methodology in this work provides more objectivity in the
5 selection of the transferrable model parameters sets for estimating the discharge at the
6 ungauged catchments. This can reduce a part of the additional uncertainty that can be
7 introduced by the user through his subjective selection of the transferrable model parameters.
8 However, some subjective choices are inevitable such as the choice of the similarity measure
9 and the selection of the catchment attributes which can have an additional source of
10 uncertainty. We think also that the speculation behinds the developed methodology such as
11 model prediction uncertainty at the ungauged catchments increases as the dissimilarity
12 between the donor and the receptor catchment increases is appealing and reasonable. The
13 method is easy and can be replicated with any model parameters transfer approach for
14 estimating flow at ungauged catchments within an uncertainty propagation framework.

15

16

17

18

19

20

21

22

23

24

25

26

27

28

1 **Acknowledgements**

2 This work was funded by the IDB (Islamic development Bank) under its Ph.D. Merit
3 Scholarship program. The work has been conducted in the context of the European project
4 CLIMB (Climate induced changes on the hydrology of Mediterranean Basins,
5 <http://www.climb-fp7.eu/home/home.php>). Authors thank Egis eau, the Syndicat Mixte du
6 Bassin du Thau and Ifremer for providing most of the data.

7

8

9

10

11

12

13

14

15

16

17

18

19

20

21

22

23

24

25

26

27

1 **References**

- 2 Abbaspour, K. C., van Genuchten, M. T., Schulin, R., and Schläppi, E.: A sequential
3 uncertainty domain inverse procedure for estimating subsurface flow and transport
4 parameters, *Water Resour. Res.*, 33, 1879-1892, doi: 10.1029/97wr01230, 1997.
- 5 Aquilina, L., Ladouche, B., Doerfliger, N., Seidel, J. L., Bakalowicz, M., Dupuy, C., and Le
6 Strat, P.: Origin, evolution and residence time of saline thermal fluids (Balaruc springs,
7 southern France): implications for fluid transfer across the continental shelf, *Chemical
8 Geology*, 192, 1-21, doi:10.1016/S0009-2541(02)00160-2, 2002.
- 9 Arabi, M., Govindaraju, R. S., and Hantush, M. M.: A probabilistic approach for analysis of
10 uncertainty in the evaluation of watershed management practices, *J. Hydrol.*, 333, 459-471,
11 doi:10.1016/j.jhydrol.2006.09.012, 2007.
- 12 Arnold, J. G., Srinivasan, R., Muttiah, R. S., and Williams, J. R.: Large area hydrological
13 modeling and assessment Part I: Model development 1, *J. Am. Water. Resour. Ass.*, 34, 73-
14 89, doi:10.1111/j.1752-1688.1998.tb05961.x, 1998.
- 15 Baghdadi, N., Cresson, R., El Hajj, M., Ludwig, R., and La Jeunesse, I.: Estimation of soil
16 parameters over bare agriculture areas from C-band polarimetric SAR data using neural
17 networks, *Hydrol. Earth Syst. Sci.*, 16, 1607-1621, doi:10.5194/hess-16-1607-2012, 2012.
- 18 Bårdossy, A.: Calibration of hydrological model parameters for ungauged catchments,
19 *Hydrol. Earth Syst. Sci.*, 11, 703-710, doi:10.5194/hess-11-703-2007, 2007.
- 20 Bastola, S., Ishidaira, H., and Takeuchi, K.: Regionalisation of hydrological model parameters
21 under parameter uncertainty: A case study involving TOPMODEL and basins across the
22 globe, *J. Hydrol.*, 357, 188-206, doi:10.1016/j.jhydrol.2008.05.007, 2008.
- 23 Beven, K., and Binley, A.: The future of distributed models: Model calibration and
24 uncertainty prediction, *Hydrol. Process.*, 6, 279-298, 1992.
- 25 Beven, K. J.: TOPMODEL: a critique, *Hydrol. Process.*, 11(9),1069–1086, 1997.
- 26 Beven, K.: On the future of distributed modelling in hydrology, *Hydrol. Process.*, 14, 3183-
27 3184, doi:10.1002/1099-1085, 2000.
- 28 Beven, K., and Freer, J.: Equifinality, data assimilation, and uncertainty estimation in
29 mechanistic modelling of complex environmental systems using the GLUE methodology, *J.
30 Hydrol.*, 249, 11-29, 2001.

- 1 Beven, K.: A manifesto for the equifinality thesis, *J. Hydrol.*, 320, 18-36,
2 doi:10.1016/j.jhydrol.2005.07.007, 2006.
- 3 Blasone, R.-S., Madsen, H., and Rosbjerg, D.: Uncertainty assessment of integrated
4 distributed hydrological models using GLUE with Markov chain Monte Carlo sampling, *J.*
5 *Hydrol.*, 353, 18-32, doi: 10.1016/j.jhydrol.2007.12.026, 2008.
- 6 Castellarin, A., Galeati, G., Brandimarte, L., Montanari, A., and Brath, A.: Regional flow-
7 duration curves: reliability for ungauged basins, *Advances in Water Resources*, 27, 953-965,
8 doi: 10.1016/j.advwatres.2004.08.005, 2004.
- 9 Chahinian, N., Tournoud, M.-G., Perrin, J.-L., and Picot, B.: Flow and nutrient transport in
10 intermittent rivers: a modelling case-study on the Vène River using SWAT 2005, *Hydrol. Sci.*
11 *J.*, 56, 268-287, doi: 10.1080/02626667.2011.559328, 2011.
- 12 Dotto, C. B., Mannina, G., Kleidorfer, M., Vezzaro, L., Henrichs, M., McCarthy, D. T., Freni,
13 G., Rauch, W., and Deletic, A.: Comparison of different uncertainty techniques in urban
14 stormwater quantity and quality modelling, *Water research*, 46, 2545-2558, doi:
15 10.1016/j.watres.2012.02.009, 2012.
- 16 Duan, Q., Sorooshian, S., and Gupta, V.: Effective and efficient global optimization for
17 conceptual rainfall-runoff models, *Water Resour. Res.*, 28, 1015-1031, doi:
18 10.1029/91wr02985, 1992.
- 19 Eckhardt, K., Fohrer, N., and Frede, H.-G.: Automatic model calibration, *Hydrol. Process.*,
20 19, 651-658, doi: 10.1002/hyp.5613, 2005.
- 21 Freer, J., Beven, K., and Ambrose, B.: Bayesian Estimation of Uncertainty in Runoff
22 Prediction and the Value of Data: An Application of the GLUE Approach, *Water Resour.*
23 *Res.*, 32, 2161-2173, doi: 10.1029/95WR03723, 1996.
- 24 Freni, G., and Mannina, G.: Bayesian approach for uncertainty quantification in water quality
25 modelling: The influence of prior distribution, *J. Hydrol.*, 392, 31-39, doi:
26 10.1016/j.jhydrol.2010.07.043, 2010.
- 27 Gallart, F., Amaxidis, Y., Botti, P., CanÈ, G., Castillo, V., Chapman, P., Froebrich, J.,
28 GarcÍA-Pintado, J., Latron, J., Llorens, P., Porto, A. L., Morais, M., Neves, R., Ninov, P.,
29 Perrin, J.-L., Ribarova, I., Skoulikidis, N., and Tournoud, M.-G.: Investigating hydrological

- 1 regimes and processes in a set of catchments with temporary waters in Mediterranean Europe,
2 *Hydrol. Sci. J.*, 53, 618-628, doi: 10.1623/hysj.53.3.618, 2008.
- 3 Gassman, P. W., Reyes, M. R., Green, C. H., and Arnold, J. G.: The Soil and Water
4 Assessment Tool: Historical development, applications and future research directions,
5 *Transactions of the ASABE*, 50, 1211-1250, 2007.
- 6 Gitau, M. W., and Chaubey, I.: Regionalization of SWAT Model Parameters for Use in
7 Ungauged Watersheds, *Water*, 2, 849-871, 2010.
- 8 Gong, Y., Shen, Z., Hong, Q., Liu, R., and Liao, Q.: Parameter uncertainty analysis in
9 watershed total phosphorus modeling using the GLUE methodology, *Agriculture, Ecosystems
10 & Environment*, 142, 246-255, doi: 10.1016/j.agee.2011.05.015, 2011.
- 11 He, Y., Bårdossy, A., and Zehe, E.: A review of regionalisation for continuous streamflow
12 simulation, *Hydrol. Earth Syst. Sci.*, 15, 3539-3553, doi: 10.5194/hess-15-3539-2011, 2011.
- 13 Heuvelmans, G., Muys, B., and Feyen, J.: Analysis of the spatial variation in the parameters
14 of the SWAT model with application in Flanders, Northern Belgium, *Hydrol. Earth Syst. Sci.*,
15 8, 931-939, 2004.
- 16 Heuvelmans, G., Muys, B., and Feyen, J.: Regionalisation of the parameters of a hydrological
17 model: Comparison of linear regression models with artificial neural nets, *J. Hydrol.*, 319,
18 245-265, doi: 10.1016/j.jhydrol.2005.07.030, 2006.
- 19 Jin, X., Xu, C.-Y., Zhang, Q., and Singh, V. P.: Parameter and modeling uncertainty
20 simulated by GLUE and a formal Bayesian method for a conceptual hydrological model, *J.
21 Hydrol.*, 383, 147-155, doi: 10.1016/j.jhydrol.2009.12.028, 2010.
- 22 La Jeunesse, I., Deslous-Paoli, J. M., Ximénès, M. C., Cheylan, J. P., Mende, C., Borrero, C.,
23 and Scheyer, L.: Changes in point and non-point sources phosphorus loads in the Thau
24 catchment over 25 years (Mediterranean Sea – France), *Hydrobiologia.*, 475-476, 403-411,
25 doi: 10.1023/a:1020351711877, 2002.
- 26 Mantovan, P., and Todini, E.: Hydrological forecasting uncertainty assessment: Incoherence
27 of the GLUE methodology, *J. Hydrol.*, 330, 368-381, doi: 10.1016/j.jhydrol.2006.04.046,
28 2006.
- 29 Masih, I., Uhlenbrook, S., Maskey, S., and Ahmad, M. D.: Regionalization of a conceptual
30 rainfall-runoff model based on similarity of the flow duration curve: A case study from the

- 1 semi-arid Karkheh basin, Iran, *J. Hydrol.*, 391, 188-201, doi: 10.1016/j.jhydrol.2010.07.018,
2 2010.
- 3 McIntyre, N., Lee, H., Wheeler, H., Young, A., and Wagener, T.: Ensemble predictions of
4 runoff in ungauged catchments, *Water Resour. Res.*, 41, W12434, doi:
5 10.1029/2005WR004289, 2005.
- 6 Merz, R., and Blöschl, G.: Regionalisation of catchment model parameters, *J. Hydrol.*, 287,
7 95-123, doi: 10.1016/j.jhydrol.2003.09.028, 2004.
- 8 Montanari, A.: Large sample behaviors of the generalized likelihood uncertainty estimation
9 (GLUE) in assessing the uncertainty of rainfall-runoff simulations, *Water Resour. Res.*, 41,
10 W08406, doi: 10.1029/2004WR003826, 2005.
- 11 Moore, R.J.: The probability-distributed principle and runoff production at point and basin
12 scales, *Hydrol. Sci. J.*, 30(2), 273-297, 1985.
- 13 Muleta, M. K., and Nicklow, J. W.: Sensitivity and uncertainty analysis coupled with
14 automatic calibration for a distributed watershed model, *J. Hydrol.*, 306, 127-145, doi:
15 10.1016/j.jhydrol.2004.09.005, 2005.
- 16 Nathan, R. J., and McMahon, T. A.: Identification of homogeneous regions for the purposes
17 of regionalisation, *J. Hydrol.*, 121, 217-238, 1990.
- 18 Neitsh, S. L., Arnold, J. G., Kiniry, J. R., Srinivasan, R., and Williams, J. R.: Soil and Water
19 Assessment Tool input/output file documentation, version 2005, Temple, Texas: Grassland,
20 Soil and Water Research Laboratory, Agricultural Research Service, 2005.
- 21 Ouarda, T. B. J. M., Girard, C., Cavadias, G. S., and Bobee, B.: Regional flood frequency
22 estimation with canonical correlation analysis, *J. Hydrol.*, 254(1-4), 157-173, 2001.
- 23 Oudin, L., Andréassian, V., Perrin, C., Michel, C., and Le Moine, N.: Spatial proximity,
24 physical similarity, regression and ungauged catchments: A comparison of regionalization
25 approaches based on 913 French catchments, *Water Resour. Res.*, 44, W03413, doi:
26 10.1029/2007WR006240, 2008.
- 27 Parajka, J., Merz, R., Blöschl, G.: A comparison of regionalisation methods for catchment
28 model parameters, *Hydrol. Earth Syst. Sci.*, 9, 157-171, 10.5194/hess-9-157-2005, 2005.
- 29 Perrin, C., Michel, C. and Andréassian, V.: Improvement of a parsimonious model for
30 streamflow simulation. *J. Hydrol.*, 279(1-4), 275-289, 2003.

- 1 Perrin, J.-L., and Tournoud, M.-G.: Hydrological processes controlling flow generation in a
2 small Mediterranean catchment under karstic influence, *Hydrol. Sci. J.*, 54, 1125-1140, doi:
3 10.1623/hysj.54.6.1125, 2009.
- 4 Plus, M., La Jeunesse, I., Bouraoui, F., Zaldivar, J., Chapelle, A., and Lazure, P.: Modelling
5 water discharges and nitrogen inputs into a Mediterranean lagoon-Impact on the primary
6 production, *Ecol. Model.*, 193, 69-89, doi: 10.1016/j.ecolmodel.2005.07.037, 2006.
- 7 Sellami, H., La Jeunesse, I., Benabdallah, S. and Vanclooster, M.: Parameter and rating curve
8 uncertainty propagation analysis of the SWAT model for two small Mediterranean
9 watersheds, *Hydrol. Sci. J.*, 58 (8):1635-1657. doi:10.1080/02626667.2013.837222, 2013.
- 10 Setegn, S. G., Srinivasan, R., Melesse, A. M., and Dargahi, B.: SWAT model application and
11 prediction uncertainty analysis in the Lake Tana Basin, Ethiopia, *Hydrol. Process.*, doi:
12 10.1002/hyp.7457, 2009.
- 13 Shen, Z. Y., Chen, L., and Chen, T.: Analysis of parameter uncertainty in hydrological
14 modeling using GLUE method: a case study of SWAT model applied to Three Gorges
15 Reservoir Region, China, *Hydrol. Earth Syst. Sci* 8, 8203-8229, doi: 10.5194/hess-8-8203-
16 2012, 2012.
- 17 Shrestha, D. L., Kayastha, N., and Solomatine, D. P.: A novel approach to parameter
18 uncertainty analysis of hydrological models using neural networks, *Hydrol. Earth Syst. Sci.*,
19 13, 1235-1248, doi: 10.5194/hess-13-1235-2009, 2009.
- 20 Shu, C. and Burn, D.H.: Spatial patterns of homogeneous pooling groups for flood frequency
21 analysis, *Hydrol. Sci. J.*, 48(4), 601-618, DOI: 10.1623/hysj.48.4.601.51417, 2003.
- 22 Sivapalan, M., Takeuchi, K., Franks, S. W., Gupta, V. K., Karambiri, H., Lakshmi, V., Liang,
23 X., McDonnell, J. J., Mendiondo, E. M., O'Connell, P. E., Oki, T., Pomeroy, J. W., Schertzer,
24 D., Uhlenbrook, S., and Zehe, E.: IAHS Decade on Predictions in Ungauged Basins (PUB),
25 2003–2012: Shaping an exciting future for the hydrological sciences, *Hydrol. Sci. J.*, 48, 857-
26 880, doi: 10.1623/hysj.48.6.857.51421, 2003.
- 27 Smakhtin, V. U.: Low flow hydrology: a review, *J. Hydrol.*, 240, 147-186, doi:
28 10.1016/S0022-1694(00)00340-1, 2001.

- 1 van Griensven, A., Meixner, T., Grunwald, S., Bishop, T., Diluzio, M., and Srinivasan, R.: A
2 global sensitivity analysis tool for the parameters of multi-variable catchment models, *J.*
3 *Hydrol.*, 324, 10-23, doi: 10.1016/j.jhydrol.2005.09.008, 2006.
- 4 van Griensven, A., Ndomba, P., Yalew, S., and Kilonzo, F.: Critical review of SWAT
5 applications in the upper Nile basin countries, *Hydrol. Earth Syst. Sci.*, 16, doi: 10.5194/hess-
6 16-3371-2012, 2012.
- 7 Vandewiele, G. L., and Elias, A.: Monthly water balance of ungauged catchments obtained by
8 geographical regionalization, *J. Hydrol.*, 170, 277-291, 1995.
- 9 Viola, F., Noto, L. V., Cannarozzo, M., and La Loggia, G.: Daily streamflow prediction with
10 uncertainty in ephemeral catchments using the GLUE methodology, *Physics and Chemistry of*
11 *the Earth, Parts A/B/C*, 34, 701-706, doi: 10.1016/j.pce.2009.06.006, 2009.
- 12 Vogel, R. M., and Fennessey, N. M.: Flow-Duration Curves 2. New Interpretation and
13 Confidence-Intervals, *J. Water Resour. Plan. Manage.*, 120, 485-504, 1994.
- 14 Vogel, R. M., and Fennessey, N. M.: Flow Duration Curve II: A review of applications in
15 water resources planning, *JAWRA, J. Am. Water Resour. Ass.*, 31, 1029-1039, doi:
16 10.1111/j.1752-1688.1995.tb03419.x, 1995.
- 17 Vrugt, J. A., ter Braak, C. J. F., Clark, M. P., Hyman, J. M., and Robinson, B. A.: Treatment
18 of input uncertainty in hydrologic modeling: Doing hydrology backward with Markov chain
19 Monte Carlo simulation, *Water Resour. Res.*, 44, doi: 10.1029/2007wr006720, 2008.
- 20 Wagener, T., and Wheeler, H. S.: Parameter estimation and regionalization for continuous
21 rainfall-runoff models including uncertainty, *J. Hydrol.*, 320, 132-154, 2006.
- 22 Wagener, T., Sivapalan, M., Troch, P., and Woods, R.: Catchment Classification and
23 Hydrologic Similarity, *Geography Compass*, 1, 901-931, doi: 10.1111/j.1749-
24 8198.2007.00039.x, 2007.
- 25 Wagener, T., Wheeler, H.S., Gupta, H.V.: *Rainfall-Runoff Modelling in Gauged and*
26 *Ungauged Catchments*, Imperial College Press, London, 300, 2004.
- 27 Xiong, L., and O'Connor, K. M.: An empirical method to improve the prediction limits of the
28 GLUE methodology in rainfall-runoff modeling, *J. Hydrol.*, 349, 115-124, 2008.

- 1 Yadav, M., Wagener, T., and Gupta, H.: Regionalization of constraints on expected watershed
2 response behavior for improved predictions in ungauged basins, *Adv. Water. Resour.*, 30,
3 1756-1774, doi: 10.1016/j.advwatres.2007.01.005, 2007.
- 4 Yang, J., Reichert, P., Abbaspour, K. C., Xia, J., and Yang, H.: Comparing uncertainty
5 analysis techniques for a SWAT application to the Chaohe Basin in China, *J. Hydrol.*, 358, 1-
6 23, doi: 10.1016/j.jhydrol.2008.05.012, 2008.
- 7 Zhang, X., Srinivasan, R., Zhao, K., and Liew, M. V.: Evaluation of global optimization
8 algorithms for parameter calibration of a computationally intensive hydrologic model, *Hydrol.*
9 *Process.*, 23, 430-441, doi: 10.1002/hyp.7152, 2009.

Table 1 Discharge and precipitation data available for each catchment

Catchment name	Discharge time period	Observations length (days)	Precipitation time period
Vène	1994-1996	667	1990-2010
Pallas	1994-1996	208	1990-2010
Lauze	NA	NA	1990-1999
Aiguilles	NA	NA	1990-1999
Joncas	2007-2009	81	1990-1999
Aygues_Vacques	2007-2009	85	1990-1999
Nègues_Vacques	NA	NA	1990-1999
Mayroual	NA	NA	1990-1999
Soupié	2007-2009	536	1990-1999
Fontanilles	2007-2009	540	1990-1999

Note: NA means not available.

Table 2 Description of the catchments attributes

Catchment name	Drainage area (Km2)	Mean elevation (m)	Average slope (%)	Vineyards (%)	Non-agr. vegetation (%)	Dominant Soil texture	Geology (surface %)
Vène	67	94.29	8.47	12.3	64	SA-L	JL-MM
Pallas	54	71.33	7	20.35	45.48	S-L	JL-MM
Lauze	9.25	64.22	8.16	8.027	64	S-L	JL-MM
Aiguilles	3.42	60	5.87	0.34	83.27	S-C-L	JL-MM
Joncas	4.14	74.45	6.56	2.5	84.22	S-C-L	JL-MM
Aygues_Vacques	12.34	29.52	3.56	14.4	37.33	S-L	MM
Nègues_Vacques	28.5	53.52	4	29.18	41.32	L	MM
Mayroual	5.1	20.45	2.55	48.63	25.15	L	MM
Soupié	15.82	43.38	3.79	35.88	45	L	MM
Fontanilles	7.4	21.21	2.38	31.39	27.11	L	MM

Note: Soil code: SA-L: sandy loam, S-L: silty loam, S-C-L: silty clayey loam and L: loam.

Geology code: JL, Jurassic Limestone; MM, Miocene Marls.

Table 3 Initial range, sensitivity analysis results and description of the selected SWAT model parameters

Parameter	Initial distribution	Parameter description [Unit]
ALPHA_BF	U [0.1 – 1]	Base-flow alpha factor [days]
GW_DELAY	U [0 – 500]	Groundwater delay [days]
GW_REVAP	U [0.02 – 0.2]	Groundwater "revap" coefficient [none]
GWQMN	U [0 – 5000]	Threshold water depth in the shallow aquifer for flow [mm]
CN2*	U [0.1 – 0.9]	Initial SCS CN II value [none]
ESCO	U [0.1 – 1]	Soil evaporation compensation factor [none]
EPCO	U [0 -1]	Plant uptake compensation factor [none]
SURLAG	U [1 – 24]	Surface runoff lag time [days]
CH_N2	U [0.1 – 0.3]	Manning's n value for main channel [none]
CH_K2	U [1 – 150]	Channel effective hydraulic conductivity [mm/hr]
SOL_AWC	U [0 – 1]	Available water capacity [mm/mm soil]
SOL_K	U [0–2000]	Soil hydraulic conductivity [mm/hr]
SOL_Z	U [0 – 3500]	Soil depth [mm]
SOL_ALB	U [0 – 1]	Moist soil albedo [none]
SLOPE*	U [0 – 0.5]	Average slope steepness [m/m]
SLSUBBSN	U [10 – 150]	Average slope length [m]
REVAPMN	U [0 – 500]	Threshold depth of water in the shallow aquifer for “revap” to occur [mm]

Note: U means uniform distribution. * Means fraction of variation by which the initial value of the parameter is changed. The rank zero is attributed to parameter that is not considered as sensitive.

1 **Table 4** Results of catchments clustering and number of Mps transferred from the donor to
 2 the receptor catchment based on the similarity measure.

	Donor catchment	Receptor catchment	Similarity	Threshold (<i>Thresh</i>)	% of Mps
Catchments cluster					
	Vène	Joncas	0.71	0.50	44.10
		Lauze	0.70	0.49	46.95
		Aiguilles	0.66	0.46	54.62
		Mayroual	0.36	0.25	89.18
	Pallas	Nègues_Vacques	0.88	0.66	16.60
		Aygues_Vacques	0.71	0.54	85.16
		Soupié	0.70	0.53	86.47
		Fontanilles	0.50	0.38	96.52

3 Note: the %Mps corresponds to the percentage of the transferred Mps out of 10,000.

4

5

6

7

8

9

10

11

12

13

14

15

16

17

18

19

1 **Table 5** Measure of the *ASRIL* factor of the predicted FDCs uncertainty intervals in the
 2 ungauged catchments

Ungauged catchment	Donor catchment	
	Vène	Pallas
Lauze	0.018	-----
Aiguilles	0.031	-----
Joncas	0.019	-----
Mayroual	0.207	-----
Fontanilles	-----	0.196
Aygues_Vacques	-----	0.117
Nègues_Vacques	-----	0.113
Soupié	-----	0.169

3

4

5

6

7

8

9

10

11

12

13

14

15

16

1 **Table 6** Statistical criteria of the regionalization approach results

Catchment	Aygues_Vacques	Soupié	Fontanilles	Joncas
NS	0.169	-0.131	-0.144	0.518
<i>P_factor</i> (%)	18	65	73	87

2
3
4
5
6
7
8
9
10
11
12
13
14
15
16
17
18
19
20
21
22

1 **Table 7** Statistical criteria of the 95% confidence “observed” and predicted soil moisture
 2 values on the three dates at the Thau catchment

Date	“Observed” soil moisture (cm ³ /cm ³)			Predicted soil moisture (cm ³ /cm ³)		
	11/18/2010	12/04/2010	12/12/2010	11/18/2010	12/04/2010	12/12/2010
Prec.*	2.2	0.6	0	2.2	0.6	0
Min-Max	0.08-0.27	0.10-0.26	0.03-0.19	0.08-0.33	0.04-0.30	0.01-0.28
Median	0.167	0.162	0.07	0.142	0.102	0.07
Mean	0.169	0.166	0.08	0.167	0.127	0.09

3 Note: *Prec. is the cumulative precipitation in (mm) from the 3 previous days to the selected
 4 date.

5

6

7

8

9

10

11

12

13

14

15

16

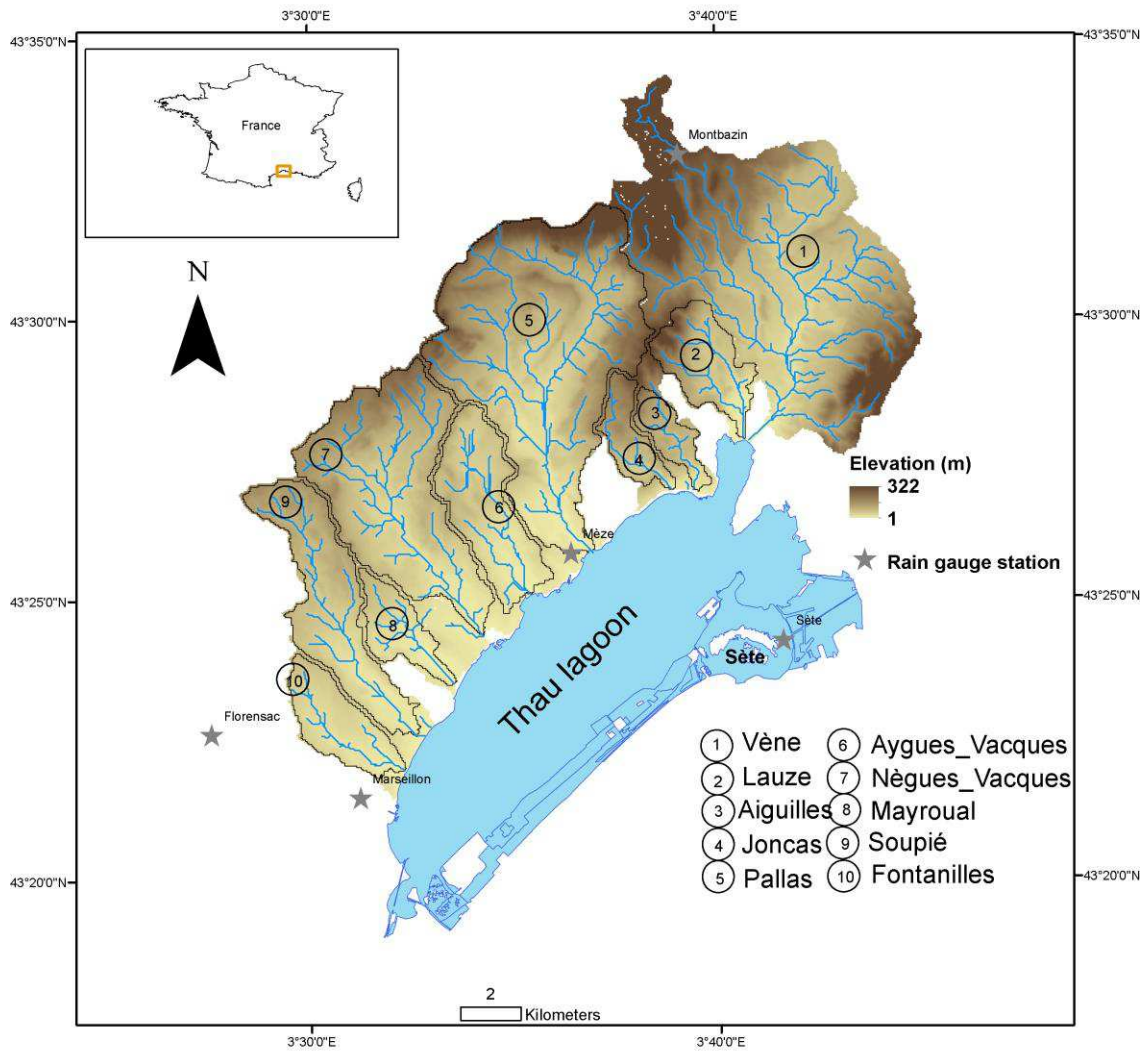
17

18

19

20

21



1

2 **Fig. 1.** Location, topography, rain gauge stations and subcatchment boundaries of the Thau
 3 basin

4

5

6

7

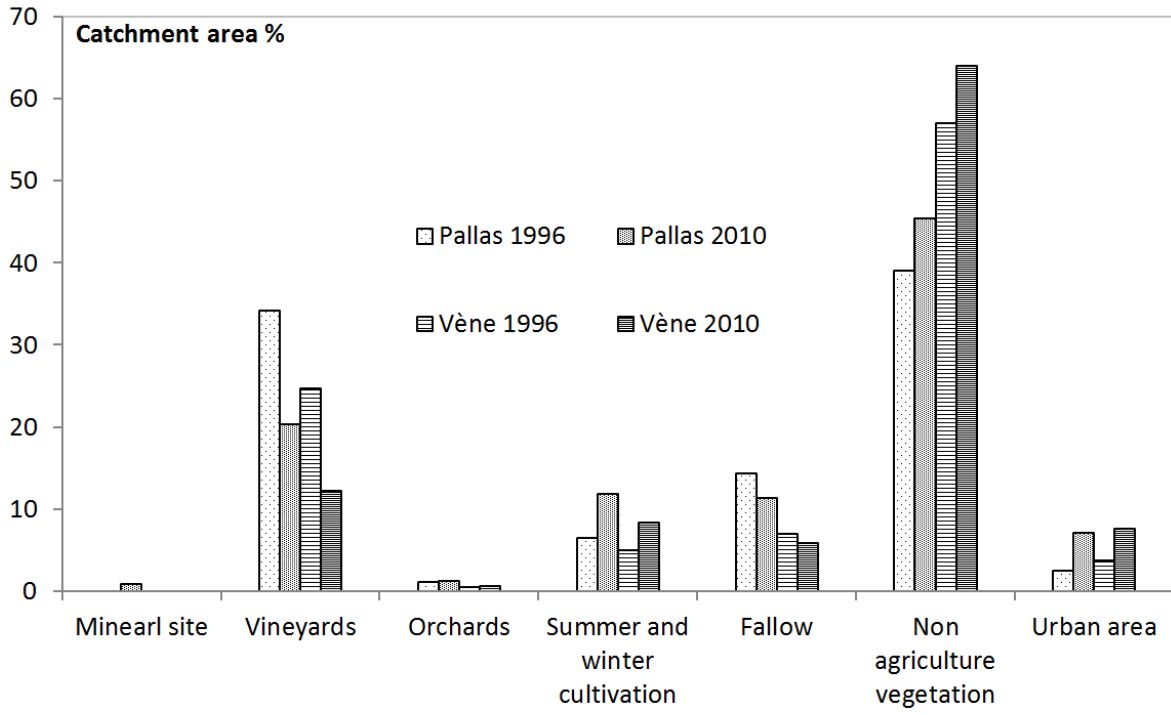
8

9

10

11

12



1

2 **Fig. 2.** Land use distribution in the Vène and in the Pallas watersheds for 1996 and 2010

3

4

5

6

7

8

9

10

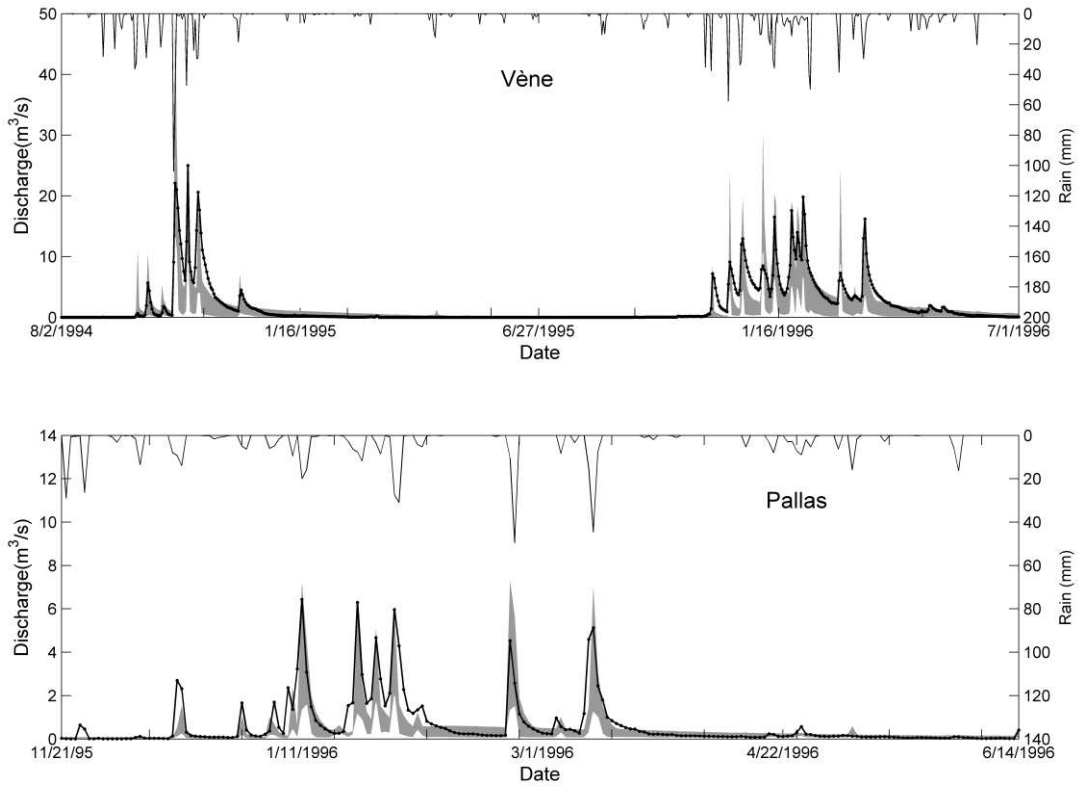
11

12

13

14

15



1

2 **Fig. 3.** GLUE prediction uncertainty bounds for the Vène and the Pallas catchment. The grey
3 shaded area is the 95% prediction uncertainty interval and the black dotted line corresponds to
4 the observed discharge

5

6

7

8

9

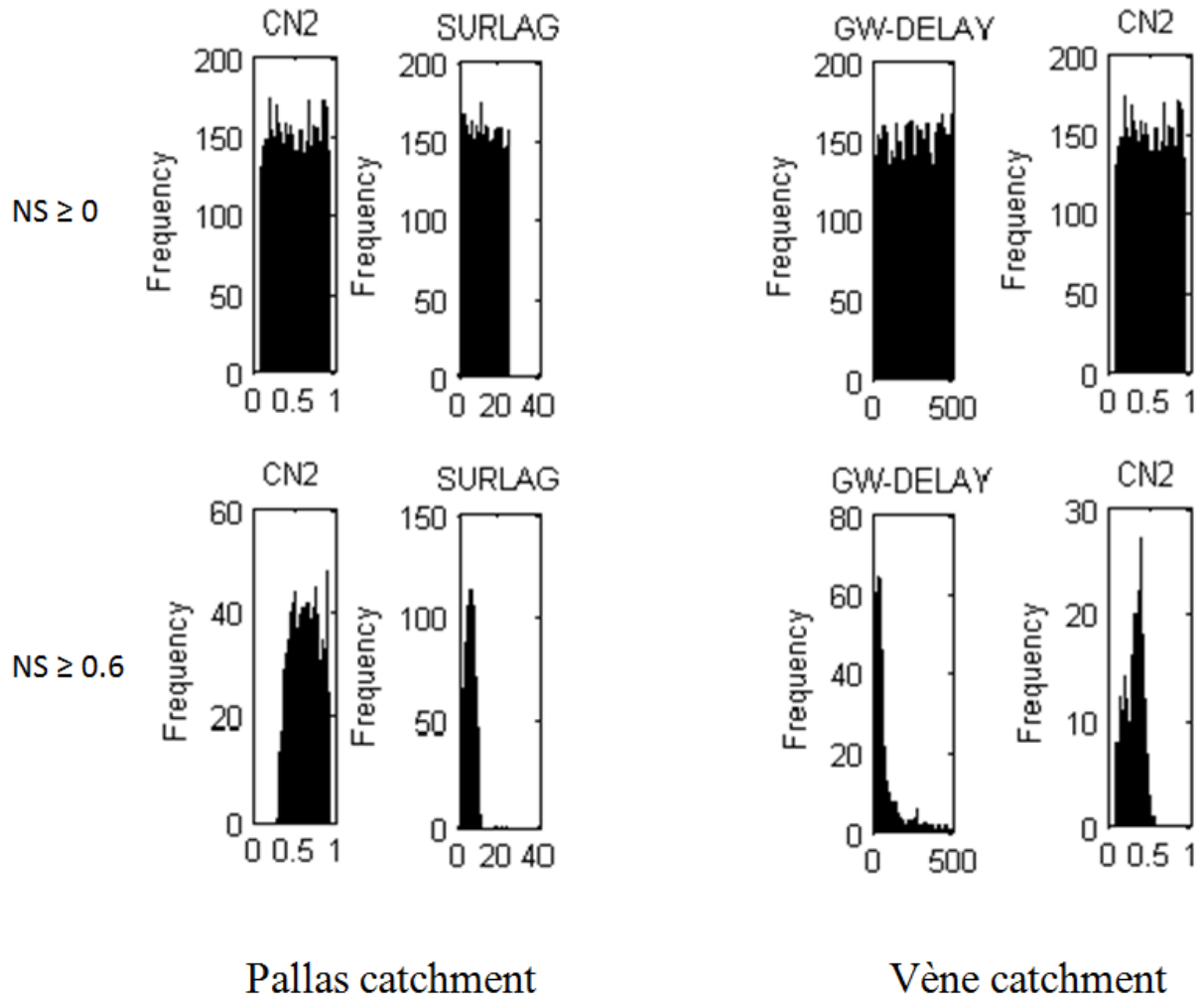
10

11

12

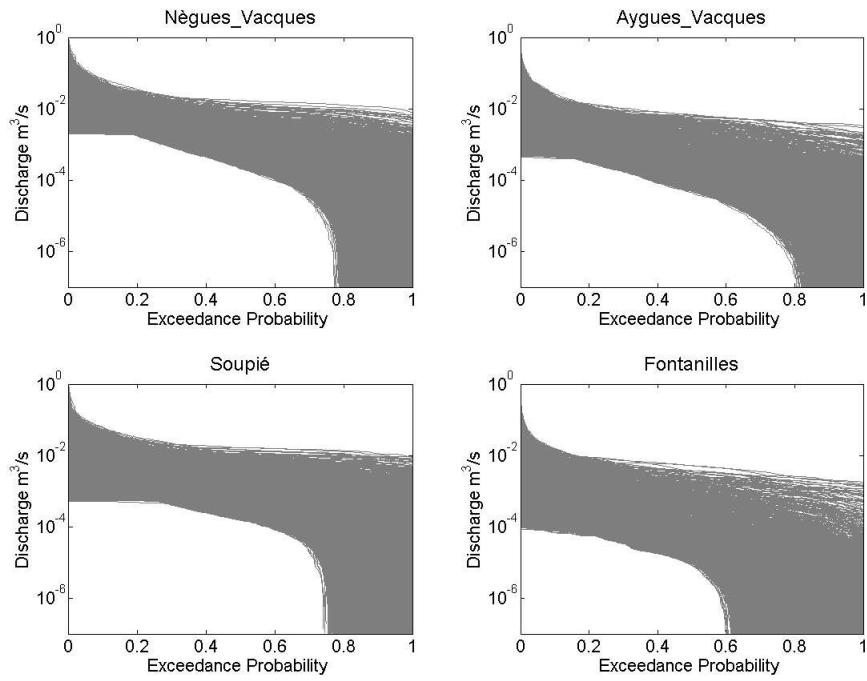
13

14



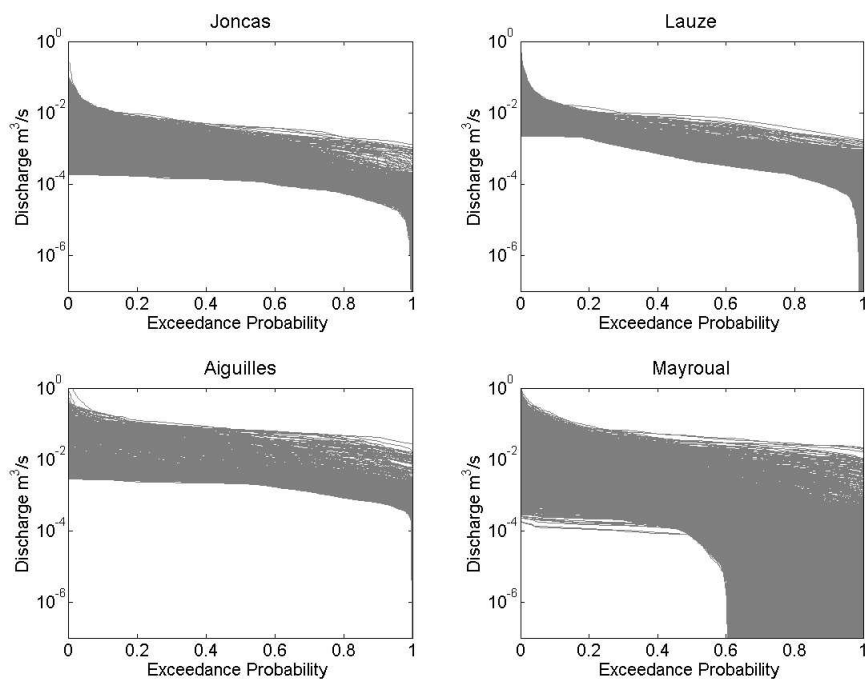
1
2
3
4
5
6
7
8
9
10
11
12

Fig. 4. Example of the effect of the threshold value on the posterior parameter distribution derived by GLUE.



1
2

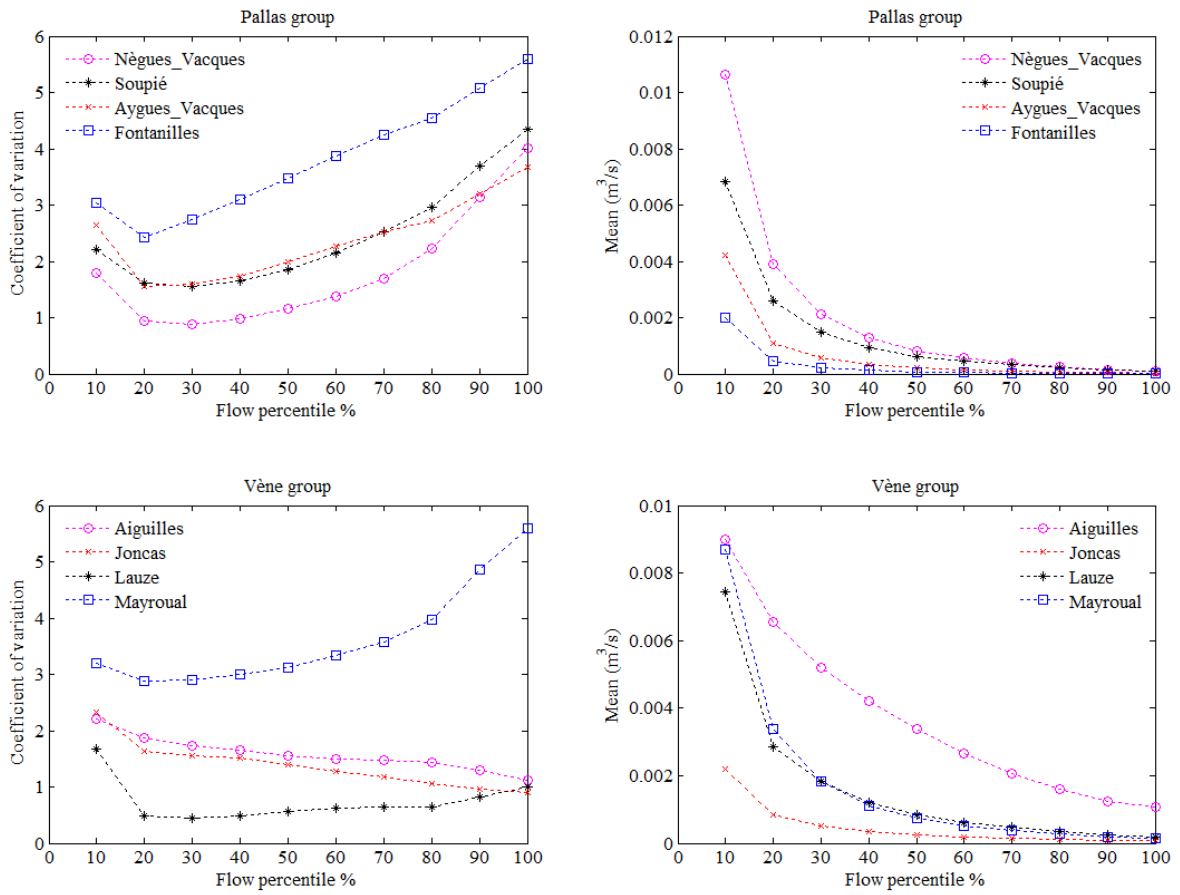
(a) Uncertain simulated FDCs for the Pallas catchments group



3
4
5

(b) Uncertain simulated FDCs for the Vène catchments group

6 **Fig. 5.** Simulated uncertain FDCs for the ungauged catchments based on model parameters
7 regionalization



1

2 **Fig. 6.** Mean and coefficient of variation of the predicted FDCs percentiles based on the
 3 physical similarity approach for the Pallas catchments group (Pallas) and for the Vène
 4 catchments group (Vène).

5

6

7

8

9

10

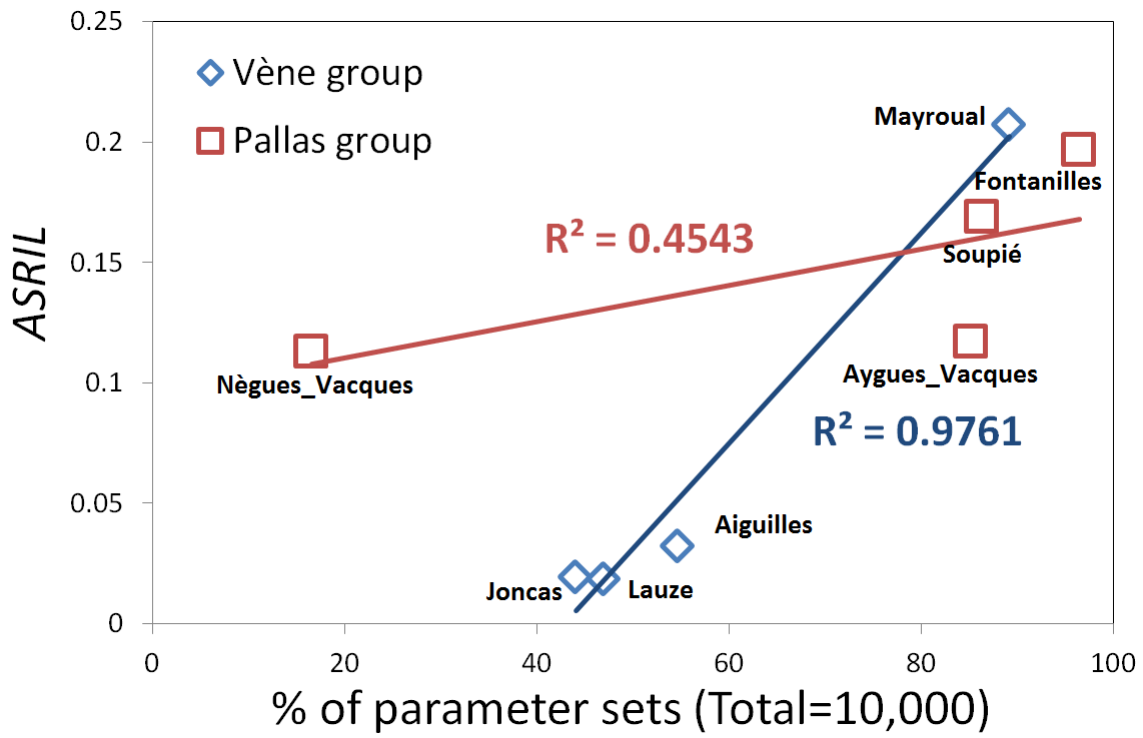
11

12

13

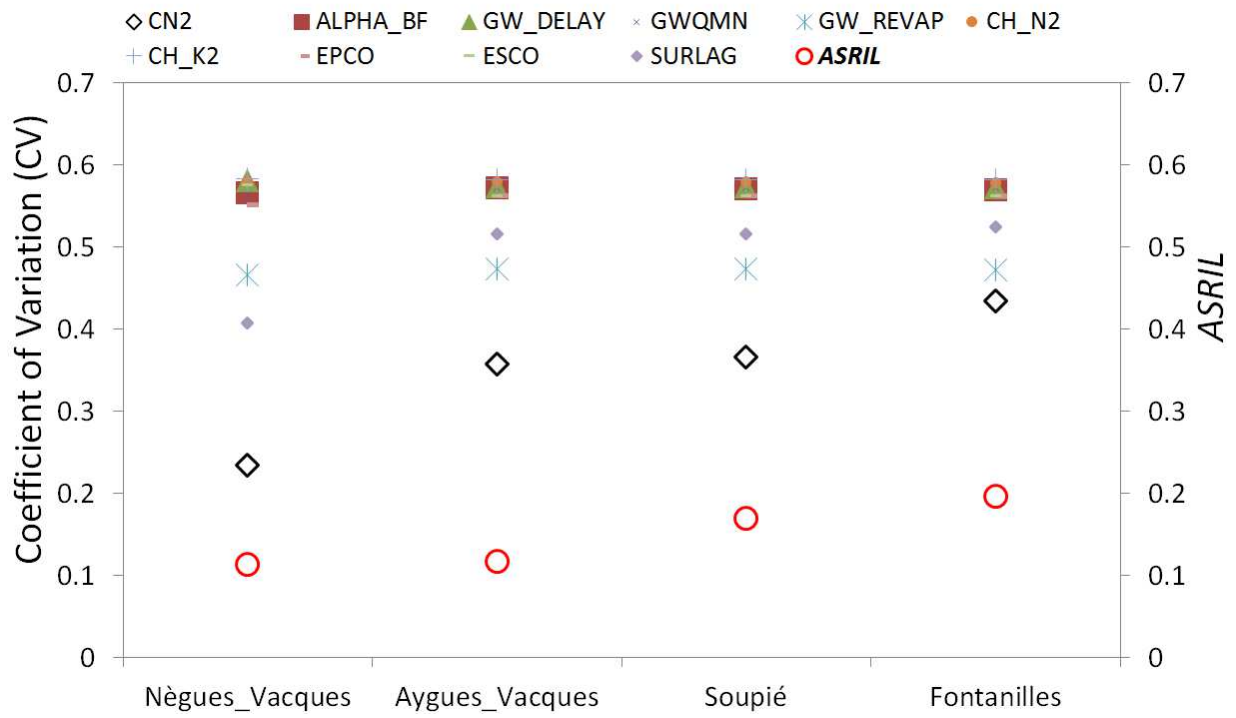
14

15

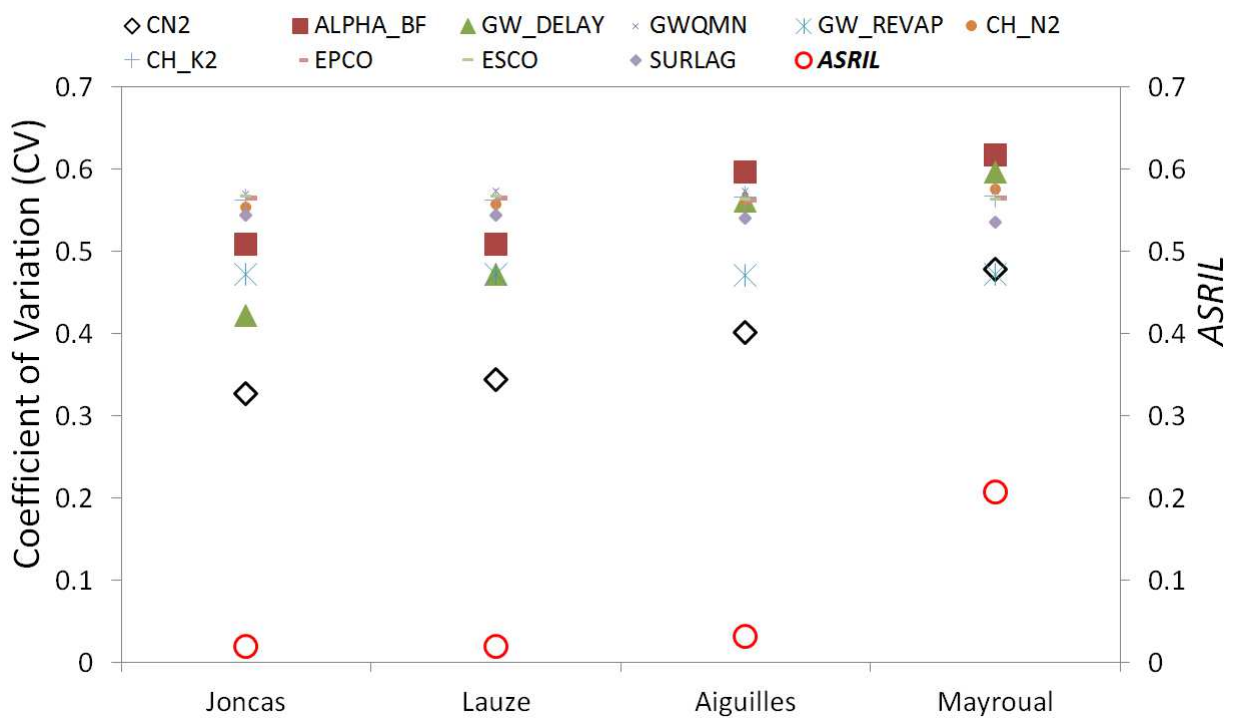


1
2
3
4
5
6
7
8
9
10
11
12
13
14
15
16
17
18

Fig. 7. Relationship between the number of transferred model parameter sets and the *ASRIL* factor at the ungauged catchments.

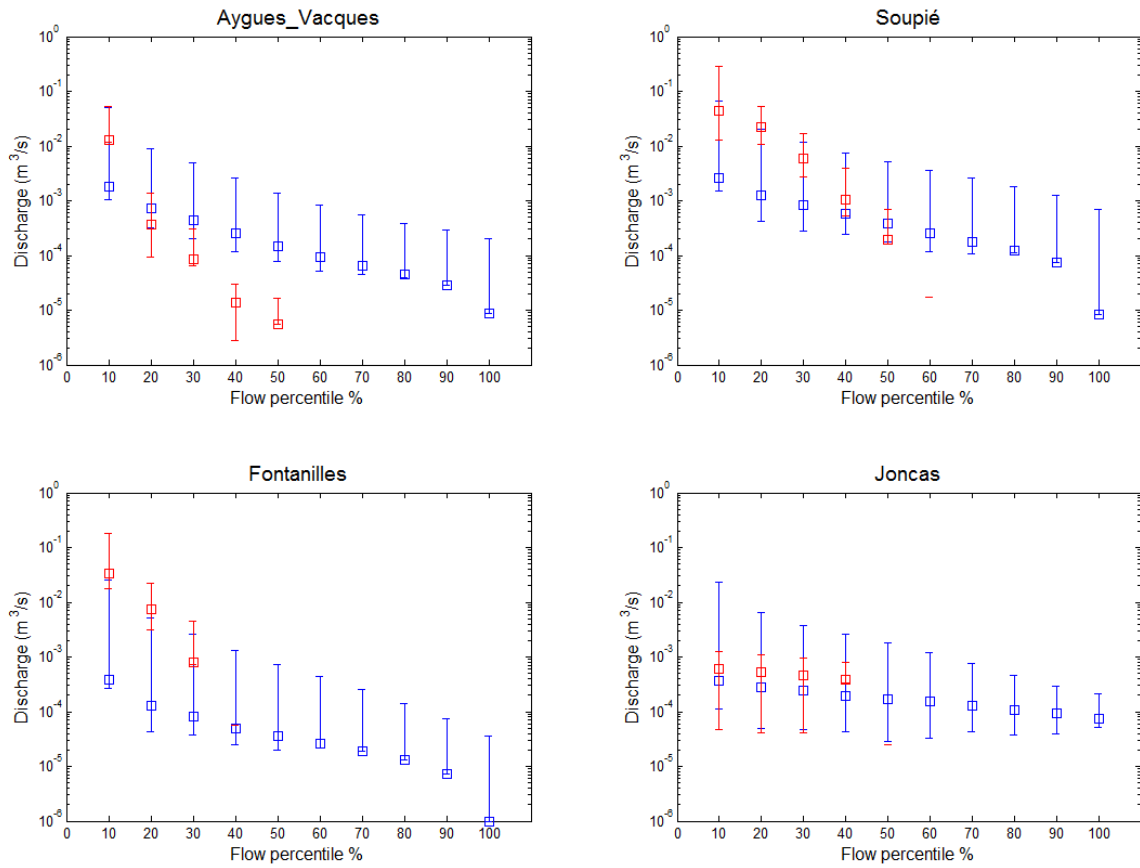


(a) Pallas catchments group



(b) Vène catchments group

Fig. 8. Relationship between the CV variability of the transferred model parameter from gauged to the ungauged catchments and the *ASRIL* factor within each catchments group.



1

2 **Fig. 9.** 95% uncertainty interval of the simulated FDCs flow percentiles versus 95% of the
 3 observed FDCs flow percentiles resulting from the model parameters regionalization
 4 approach. Results correspond to the transfer of the Pallas model parameter sets to the
 5 Aygues_Vacques, Soupié and Fontanilles catchments and transfer of the Vène model
 6 parameters sets to the Joncas catchments. The blue color is for simulation and the red color is
 7 for observation. The bar corresponds to the 95% flow percentile value while the square
 8 corresponds to the flow percentile median value.

9

10

11

12

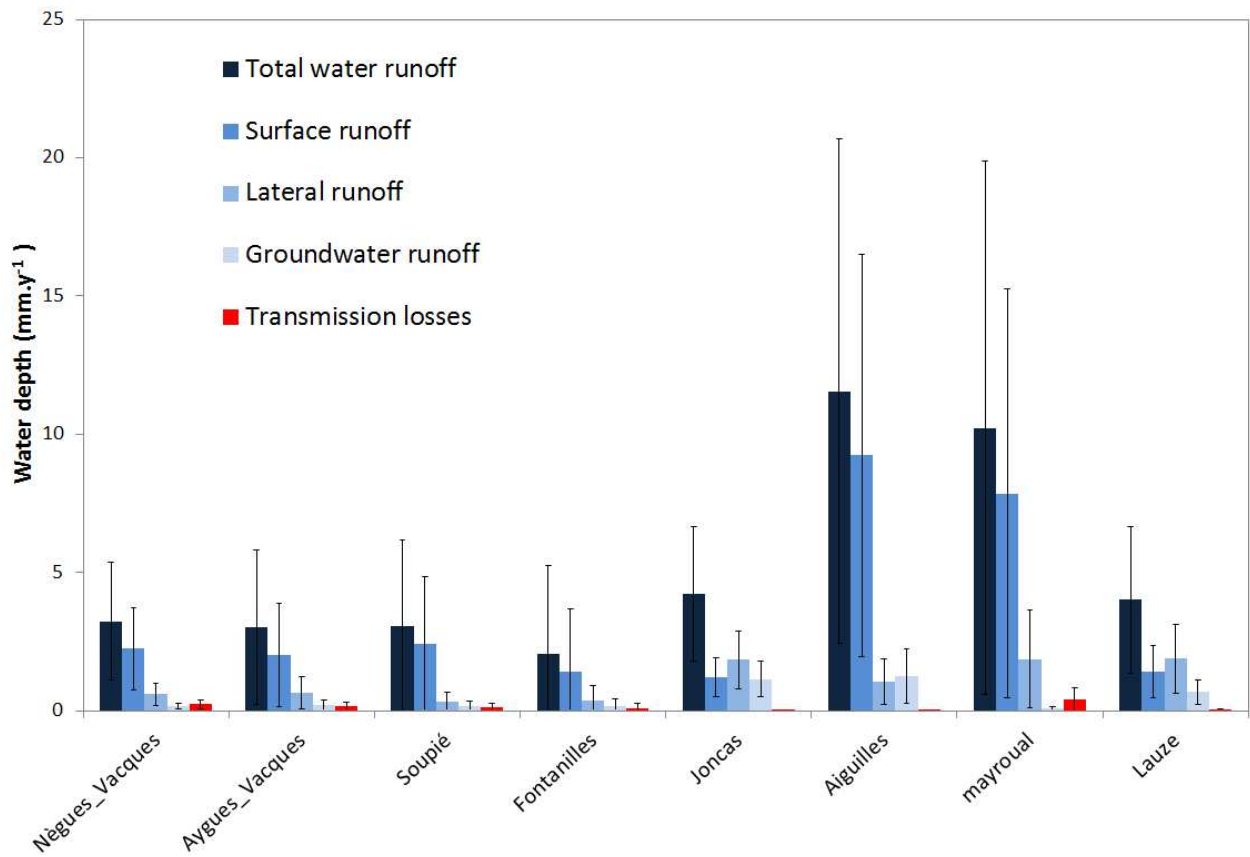
13

14

15

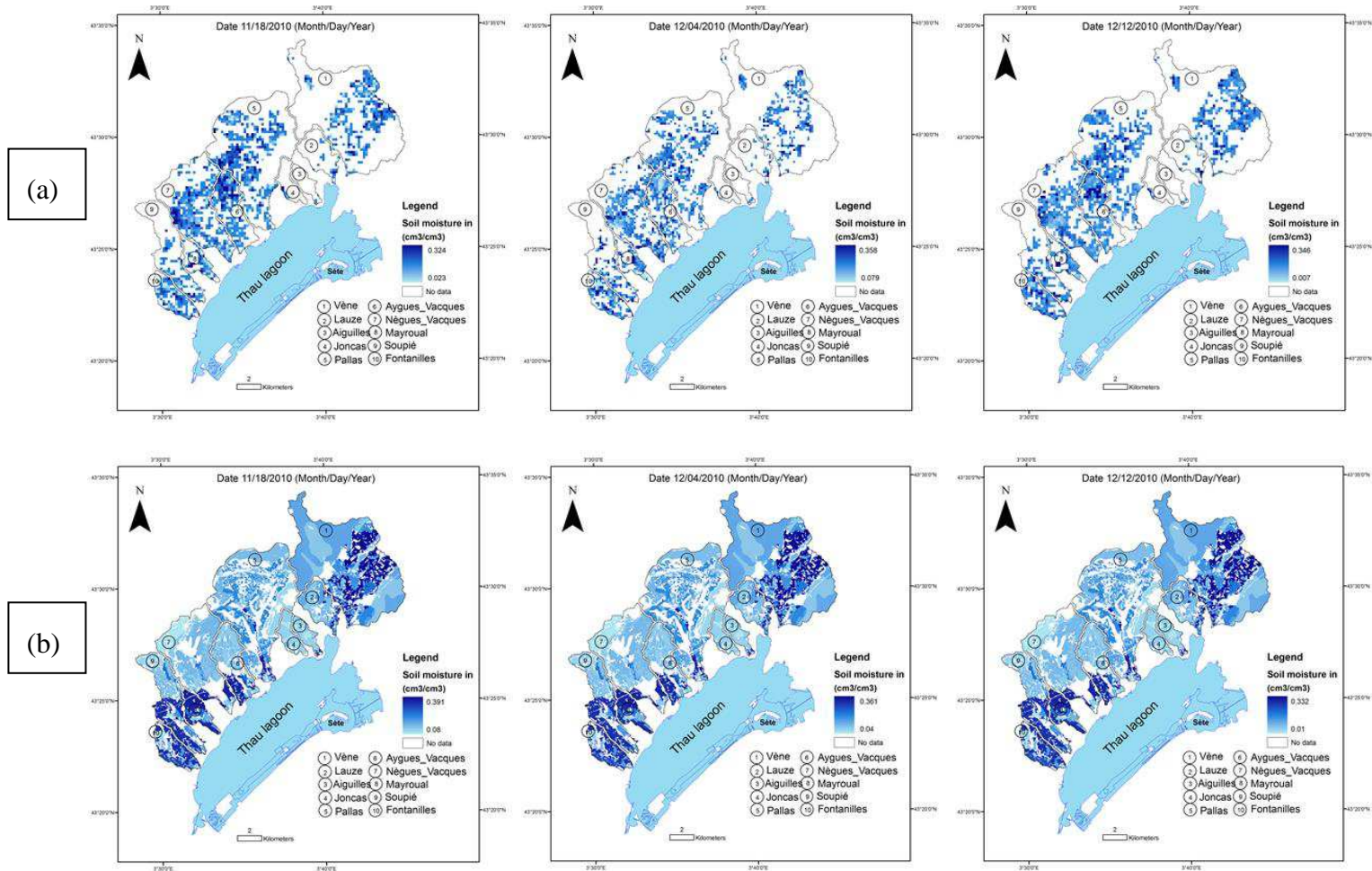
16

17



1
2
3
4
5
6
7
8
9
10
11
12
13
14
15
16

Fig. 10. Average annual water balance simulated at the ungauged catchments based on the regionalization approach. The error bars represent the standard deviation calculated based on all model simulations.



1

2

3 **Fig. 11.** Distribution of the soil moisture within the Thau catchment for 3 different dates; (a) is the “observed” soil moisture (Baghdadi et al.,
 4 2012) and (b) is the predicted soil moisture based on the regionalization results.

5